Electronic Supporting Information

for

# Structural diversity in 1D hydrogen-bonded chains assembled through bis(triazole) self–association

Jordan N. Smith[a] and Nicholas G. White[*a]

[a] Research School of Chemistry, Australian National University, Canberra, ACT, 2601, Australia
Email: nicholas.white@anu.edu.au Web: www.nwhitegroup.com

Table of Contents

## 1. SYNTHESIS & CHARACTERISATION

All commercially purchased starting materials were used as received. $^{1}$H and $^{13}$C NMR spectra were recorded in 5 mm diameter tubes at 25 °C, on a Bruker Avance 400 MHz spectrometer, and $^{1}$H and $^{13}$C NMR resonances were referenced against residual non-perdeuterated solvent signals.[1] HR MS (ESI) mass spectra were acquired on a Micromass Waters ZMD ToF spectrometer.

Known precursors **S1**–**S4**,[2,3] **2**,[2] and **4**[3] (Scheme S1) were synthesised using literature methods with minor modifications and gave NMR spectra consistent with those reported previously.[2,3] Benzyl azide (**$BnN_3$**) was synthesised using the method reported by Smith.[4] Model bis(triazole) compound **5** (*i.e.* compound **3** without the methyl groups) was prepared as previously described,[5] **btp** compound **6** was prepared as previously described.[6]

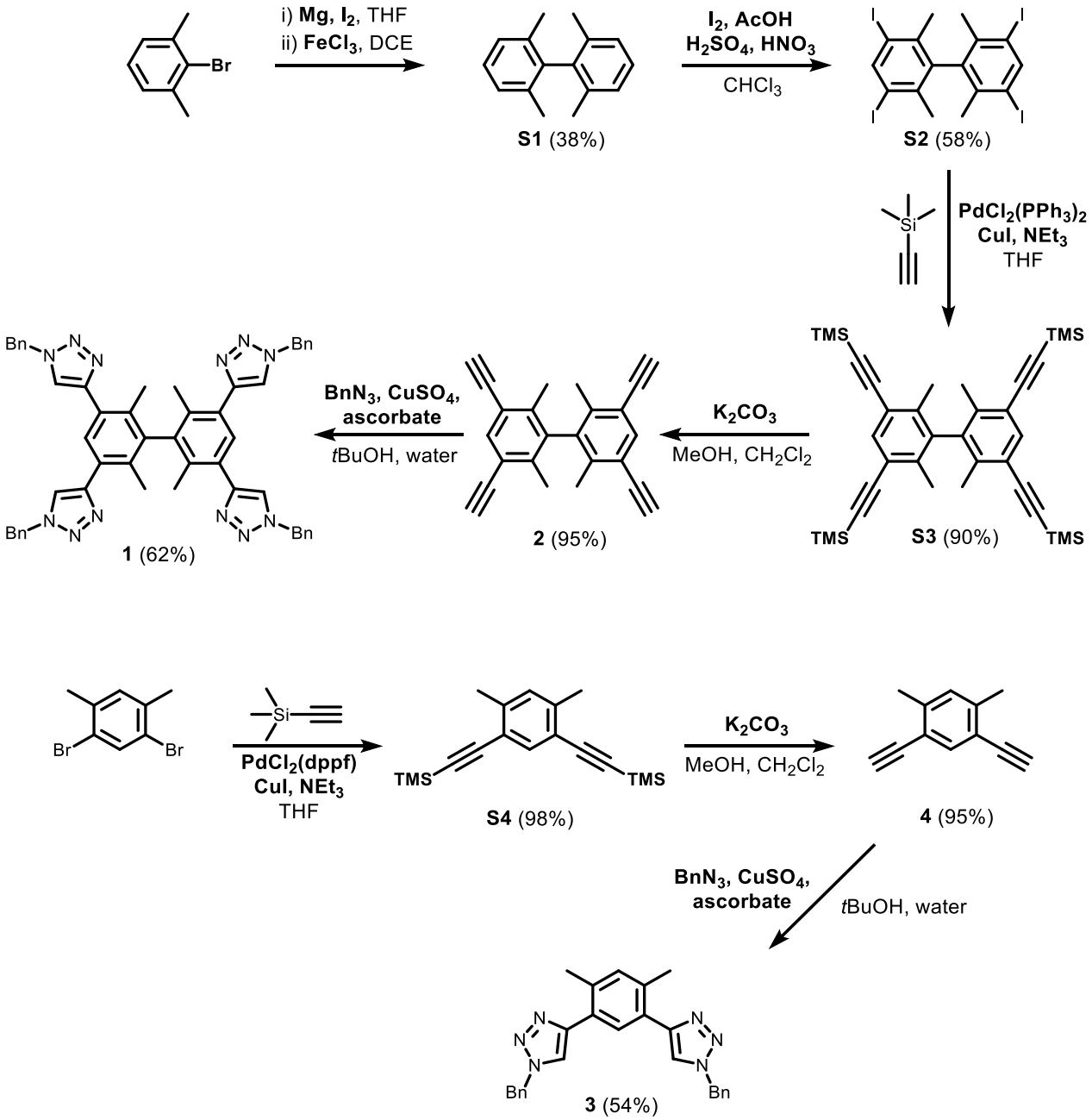


**Scheme S1.** Synthesis of ditopic tetrakis(triazole) **1** and methyl-substituted monotopic bis(triazole) **3**.

**NMR spectra of compound 1 ($CDCl_3$):**

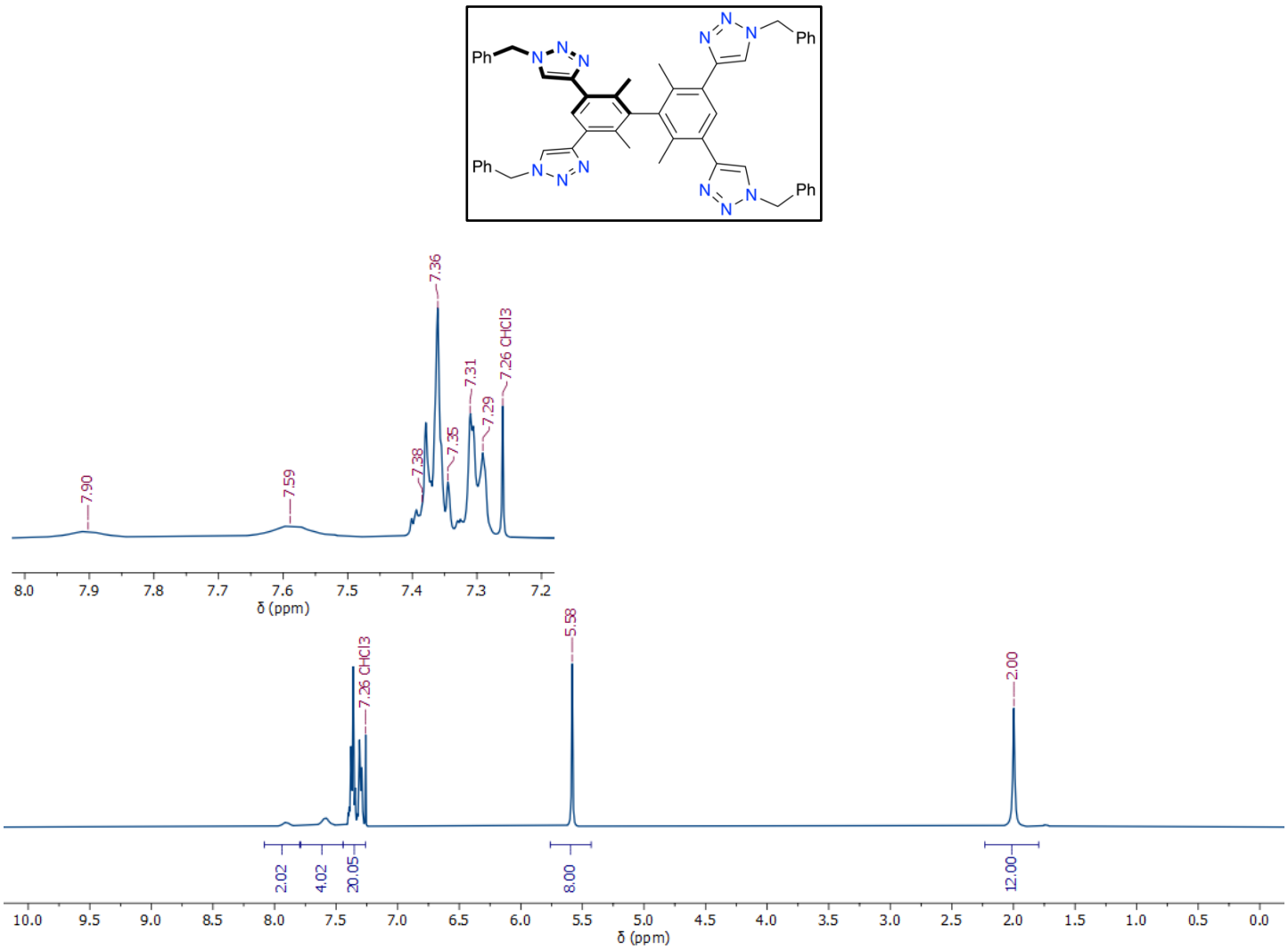


**Figure S1.** $^{1}H$ spectrum of tetrakis(triazole) compound **1** (400 MHz, 298 K, $CDCl_3$).

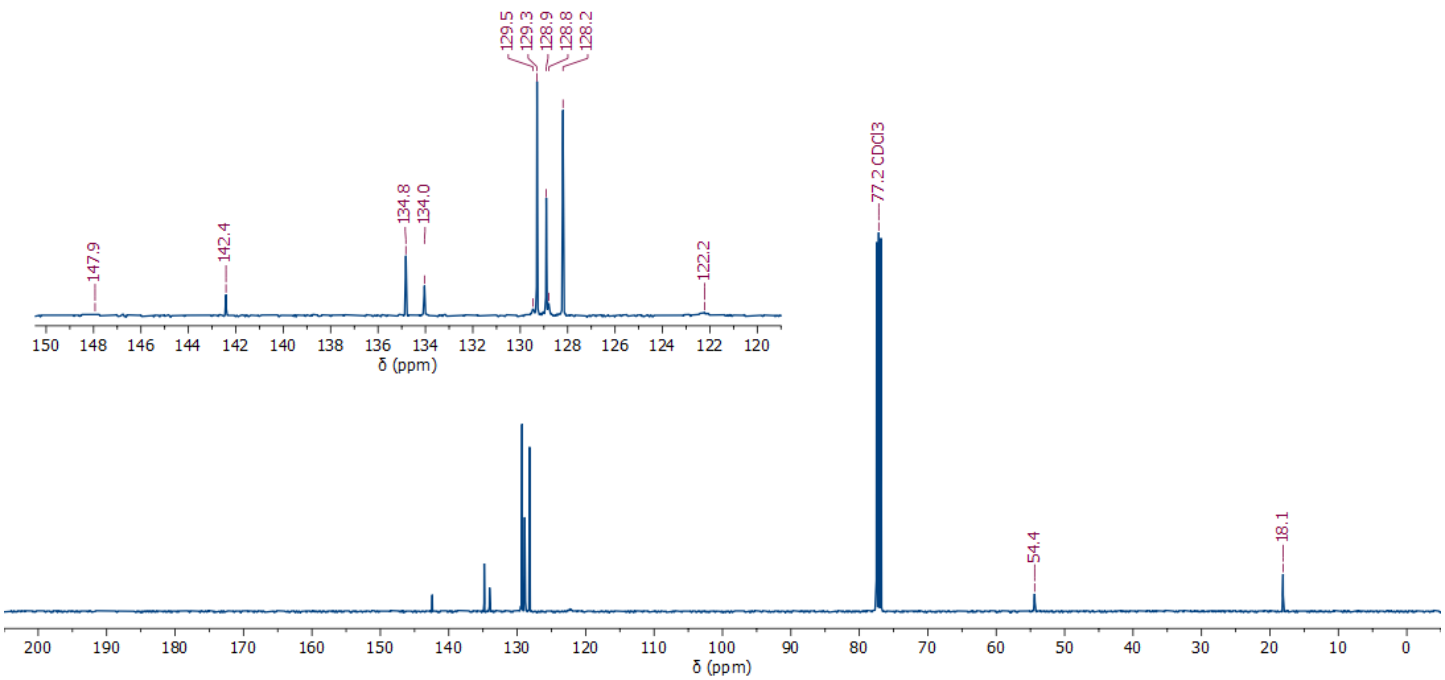


**Figure S2.** $^{13}C\{^{1}H\}$ spectrum of tetrakis(triazole) compound **1** (101 MHz, 298 K, $CDCl_3$).

**NMR spectra of compound 3 ($CDCl_3$):**

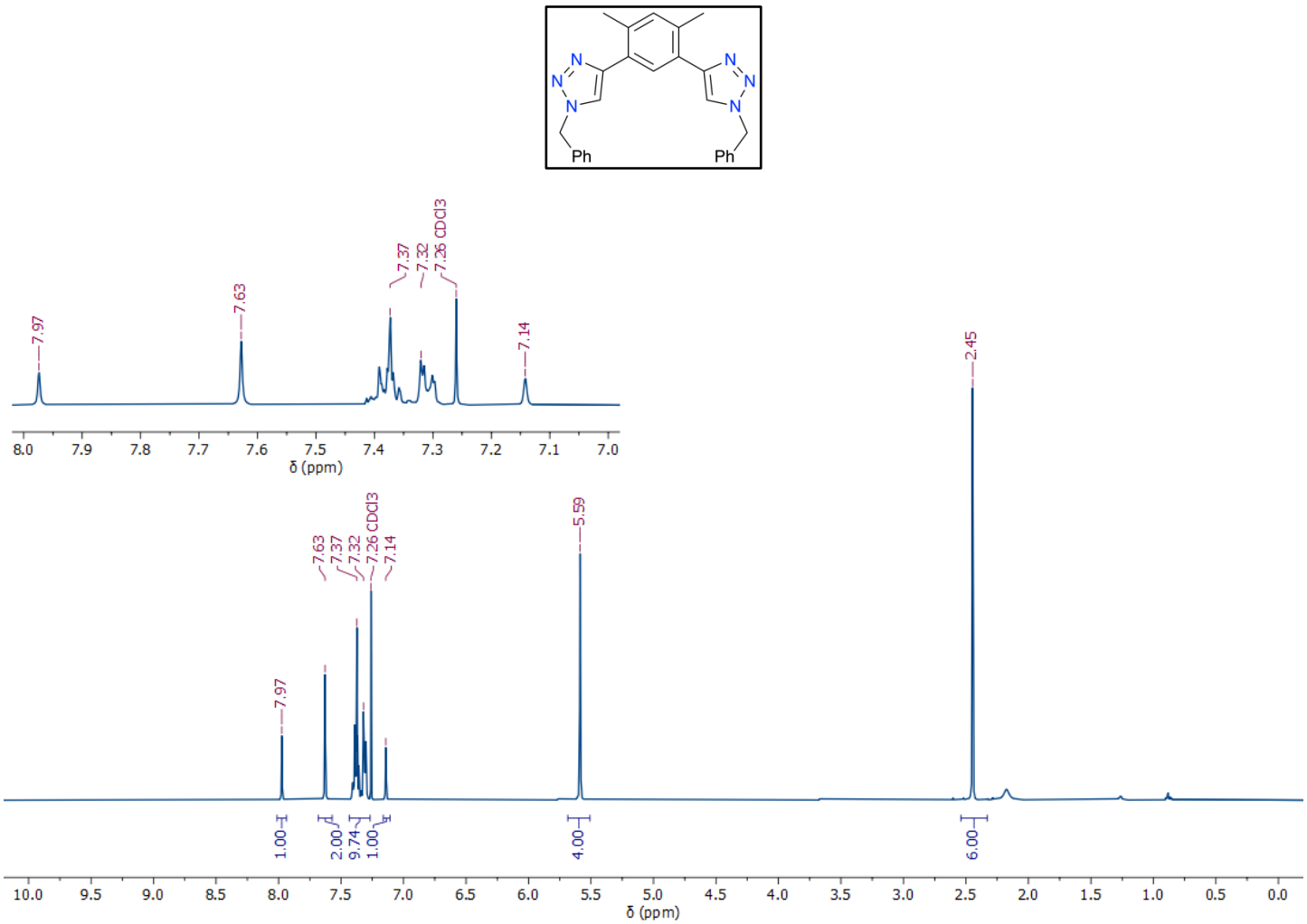


**Figure S3.** $^{1}H$ spectrum of bis(triazole) compound **3** (400 MHz, 298 K, $CDCl_3$).

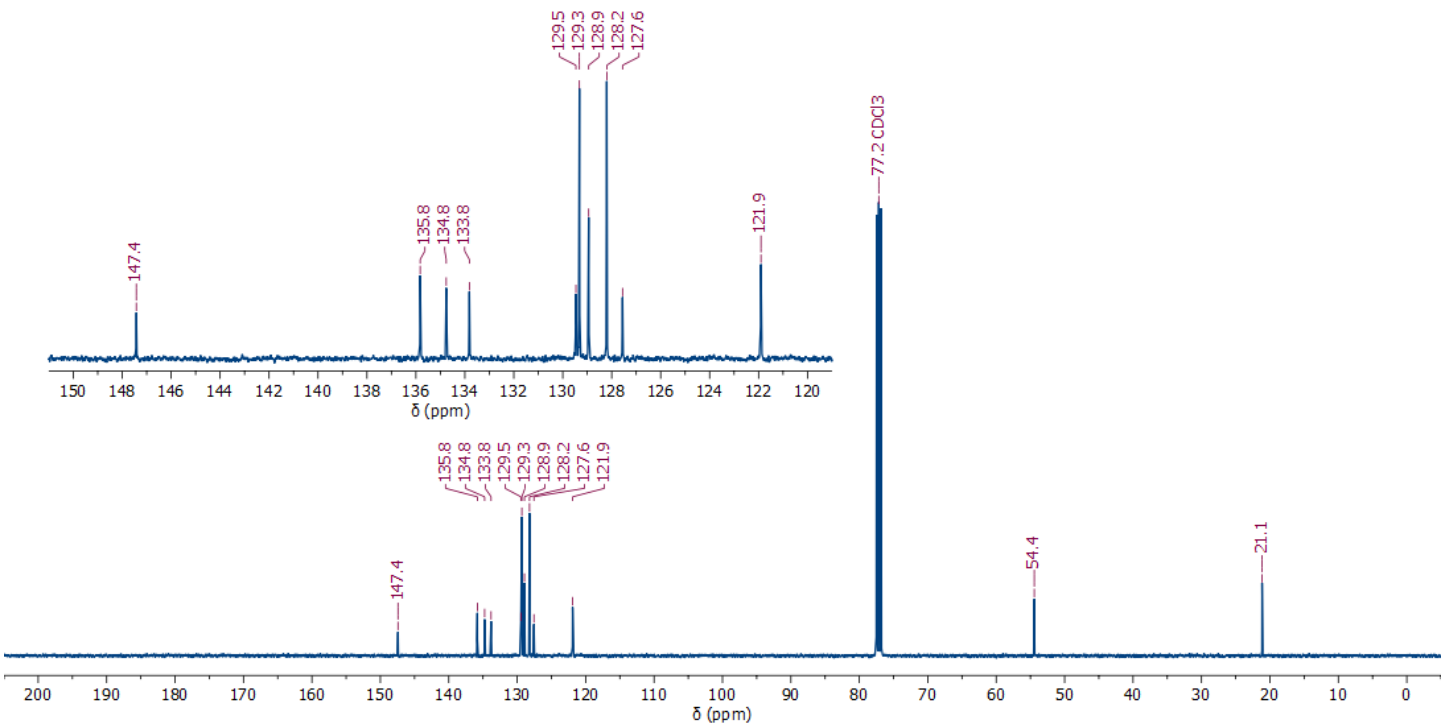


**Figure S4.** $^{13}C\{^{1}H\}$ spectrum of bis(triazole) compound **3** (101 MHz, 298 K, $CDCl_3$).

**NMR spectra of compound 8 ($d_6$-DMSO):**

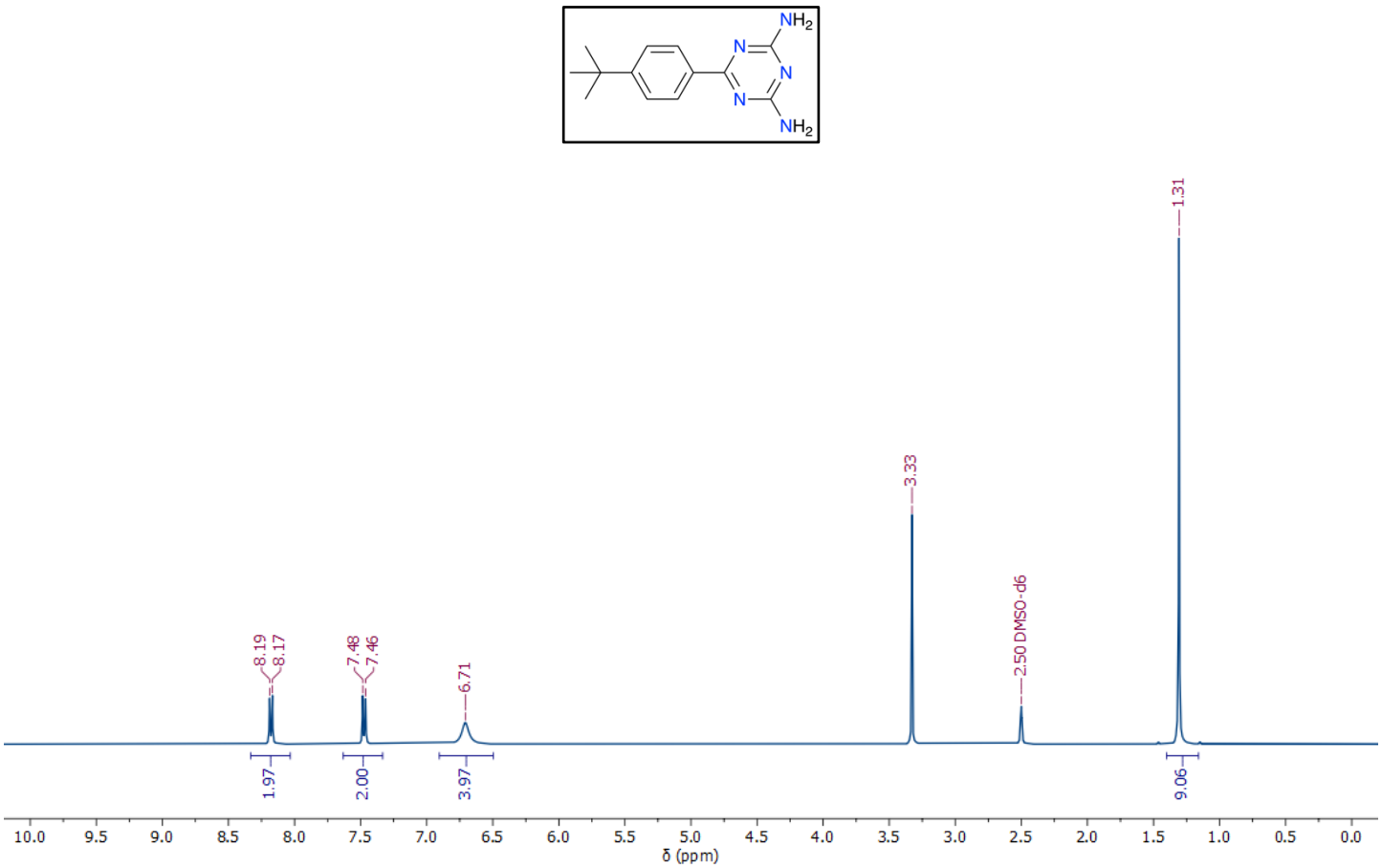


**Figure S5.** $^{1}H$ spectrum of diaminotriazine compound **8**, peak at 3.33 ppm is due to water (400 MHz, 298 K, $CDCl_3$).

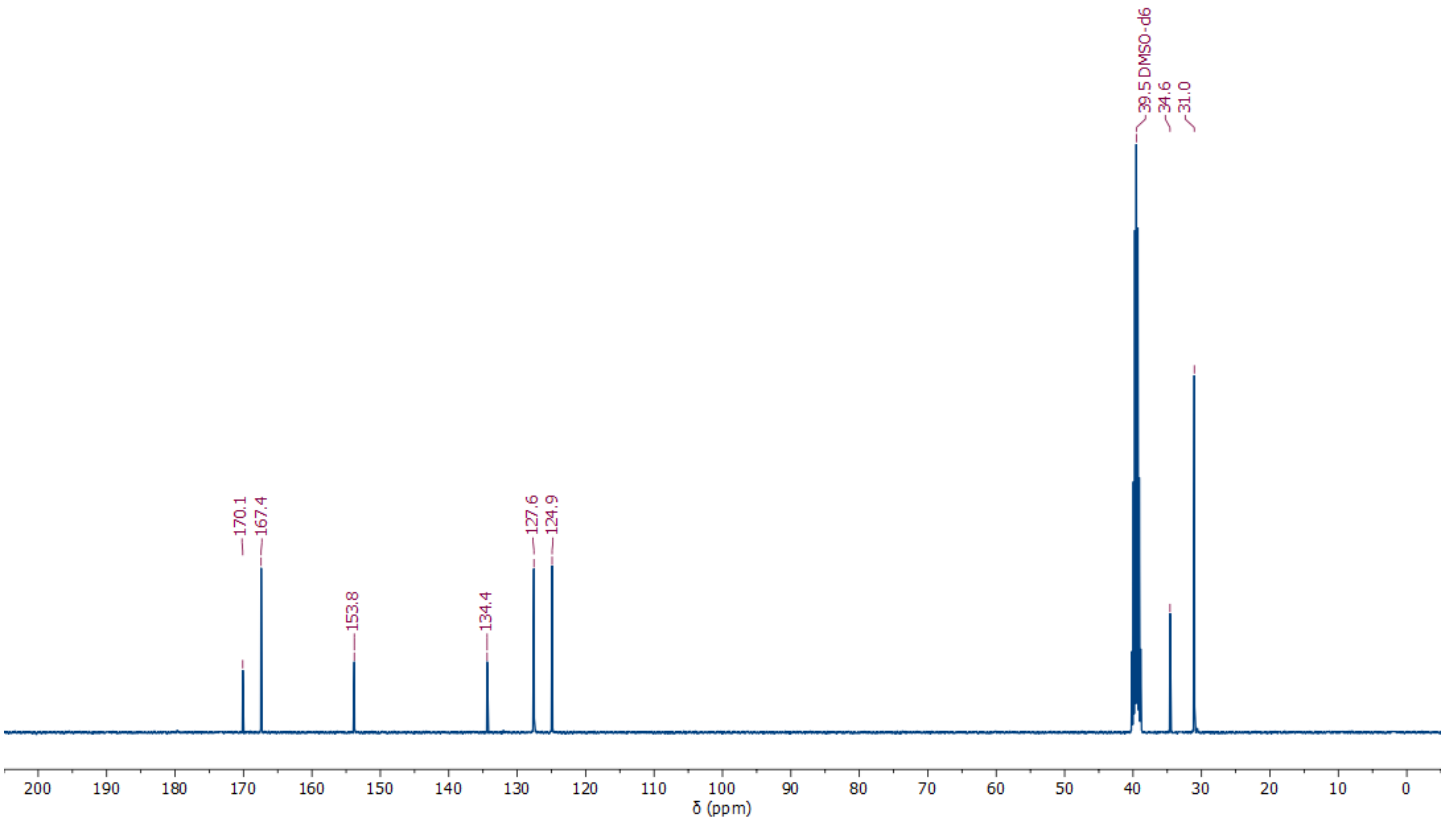


**Figure S6.** $^{13}C\{^{1}H\}$ spectrum of diamino compound **8** (101 MHz, 298 K, $CDCl_3$).

## 2. SOLUTION SELF–ASSOCIATION STUDIES

**Self–association of 3:** Solution self–association of model compound **3** was studied in $CDCl_3$, $d_6$-acetone and 9:1 v:v $CDCl_3$:$d_6$-acetone. In each case, $^1$H NMR spectra were collected at a range of concentrations. As can be seen in Figures S7 and S8, no significant change in peak position is observed in either $CDCl_3$ or $d_6$-acetone over the range of concentrations studied. In 9:1 $CDCl_3$:$d_6$-acetone, significant changes are observed (Figures S9 and S10). The peak movements of the triazole C–H and internal phenylene C–H resonances (the peaks that moved the most) were fitted using a global fit in *Bindfit*[7] to give $K_{dimerisation}$ = 4465 ± 64 $M^{-1}$ (Figure S11). Fitting these same peaks in *Musketeer* gave $K_{dimerisation}$ of 4460 $M^{-1}$ (Figure S12).

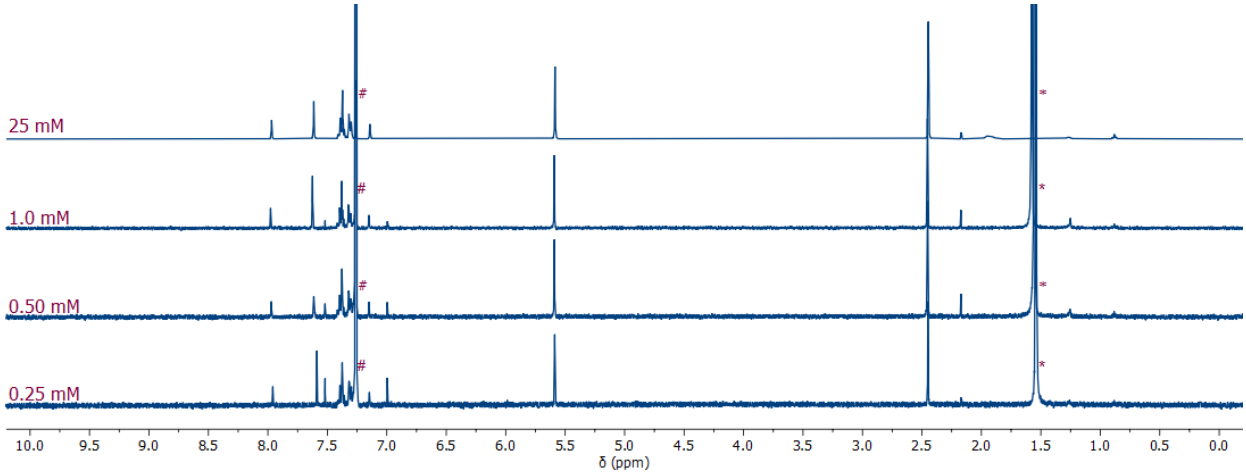


**Figure S7.** $^1$H NMR spectra of **3** at various concentrations in $CDCl_3$ (400 MHz, 298 K), * indicates incompletely deuterated NMR solvent peak, # indicates water.

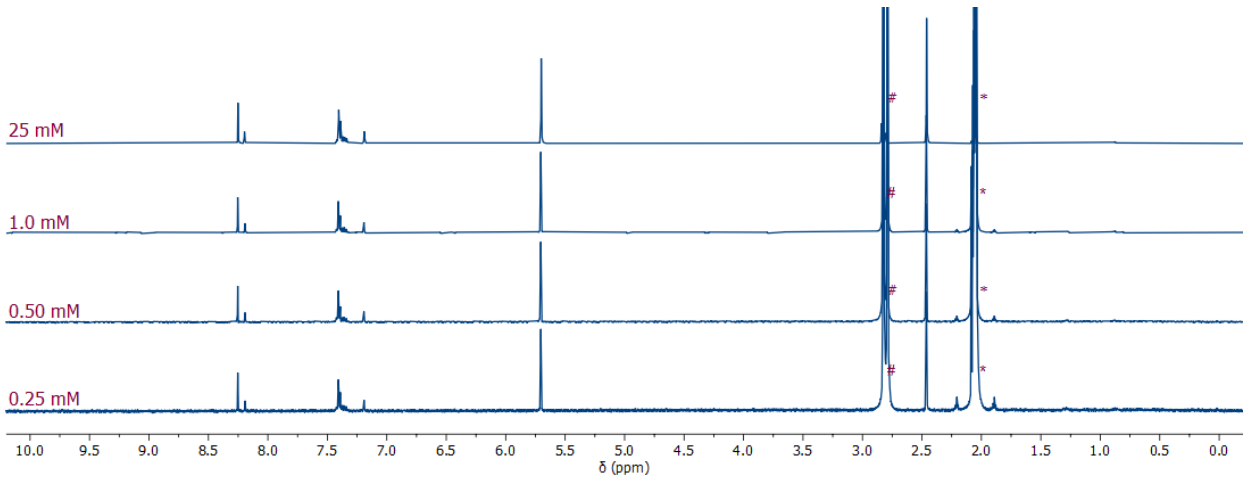


**Figure S8.** $^1$H NMR spectra of **3** at various concentrations in $d_6$-acetone (400 MHz, 298 K), * indicates incompletely deuterated NMR solvent peak, # indicates water.

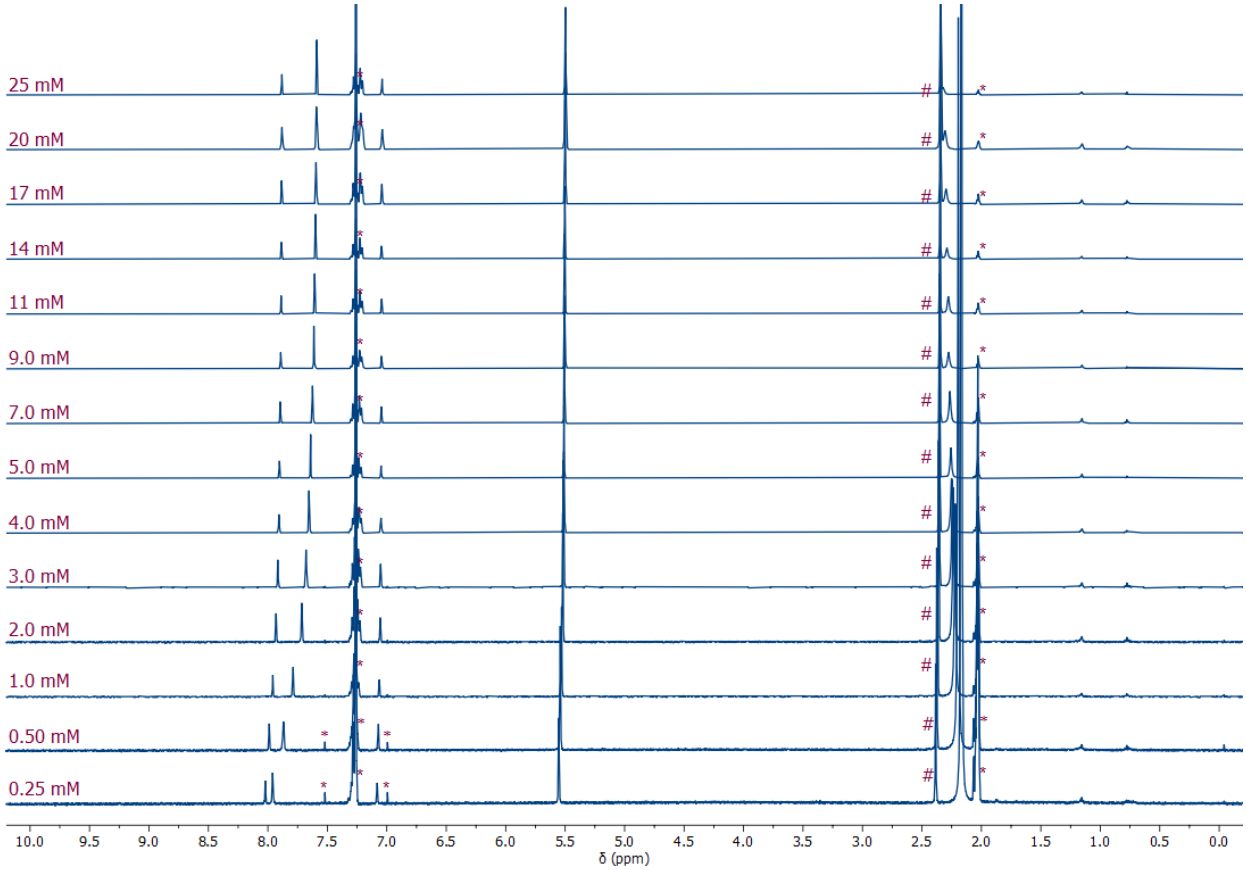


**Figure S9.** $^{1}$H NMR spectra of **3** at various concentrations in 9:1 $CDCl_3$:$d_6$-acetone (400 MHz, 298 K), * indicates incompletely deuterated NMR solvent peaks (or $^{13}$C satellites), # indicates water.

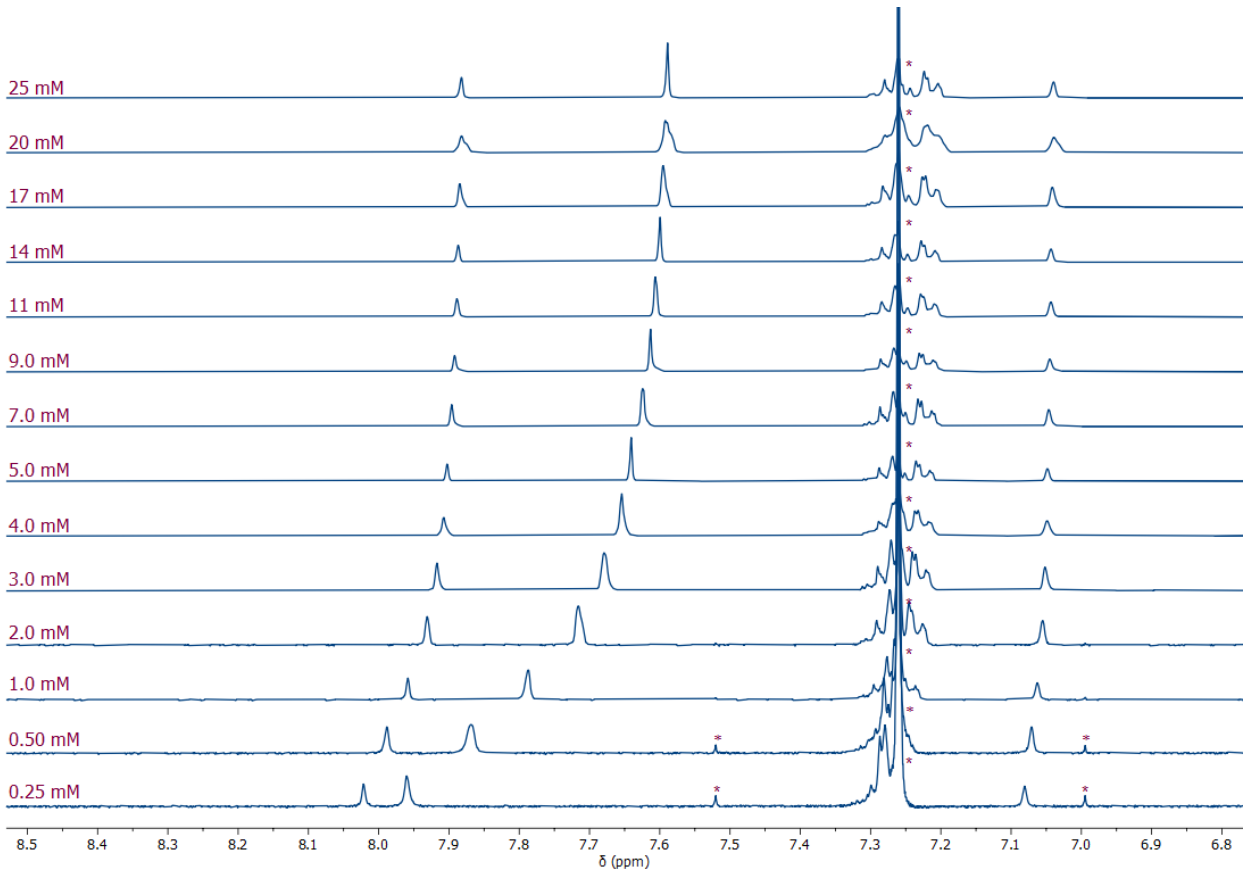


**Figure S10.** Partial $^{1}$H NMR spectra of **3** at various concentrations in 9:1 $CDCl_3$:$d_6$-acetone (400 MHz, 298 K), * indicates incompletely deuterated NMR solvent peak and $^{13}$C satellite peaks of this peak.

Full binding data including the calculated fit for this experiment can be obtained at:
http://app.supramolecular.org/bindfit/view/ad0a17ba-7151-4239-af5a-41bb7be5d40a

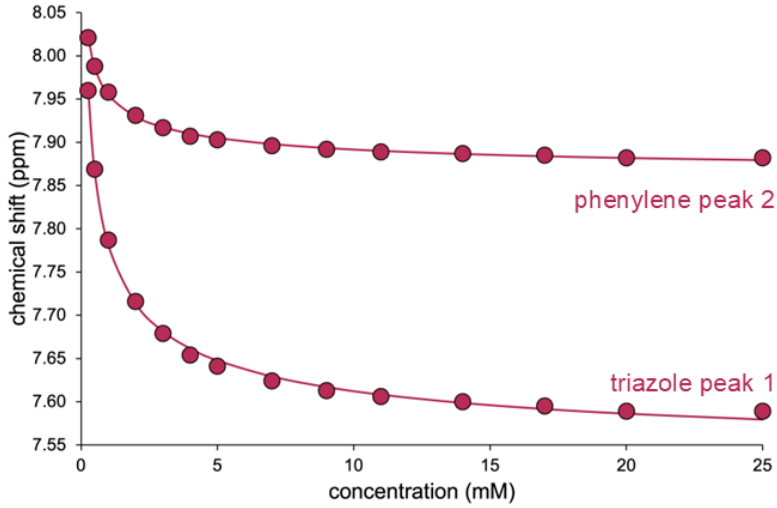


**Figure S11.** Chemical shift of interior phenylene and triazole C–H resonances of **3** at various concentrations; circles represent data, lines represent dimerization isotherm calculated using *Bindfit*[7] ($K_{dimerisation}$ = 4465 ± 64 $M^{-1}$).

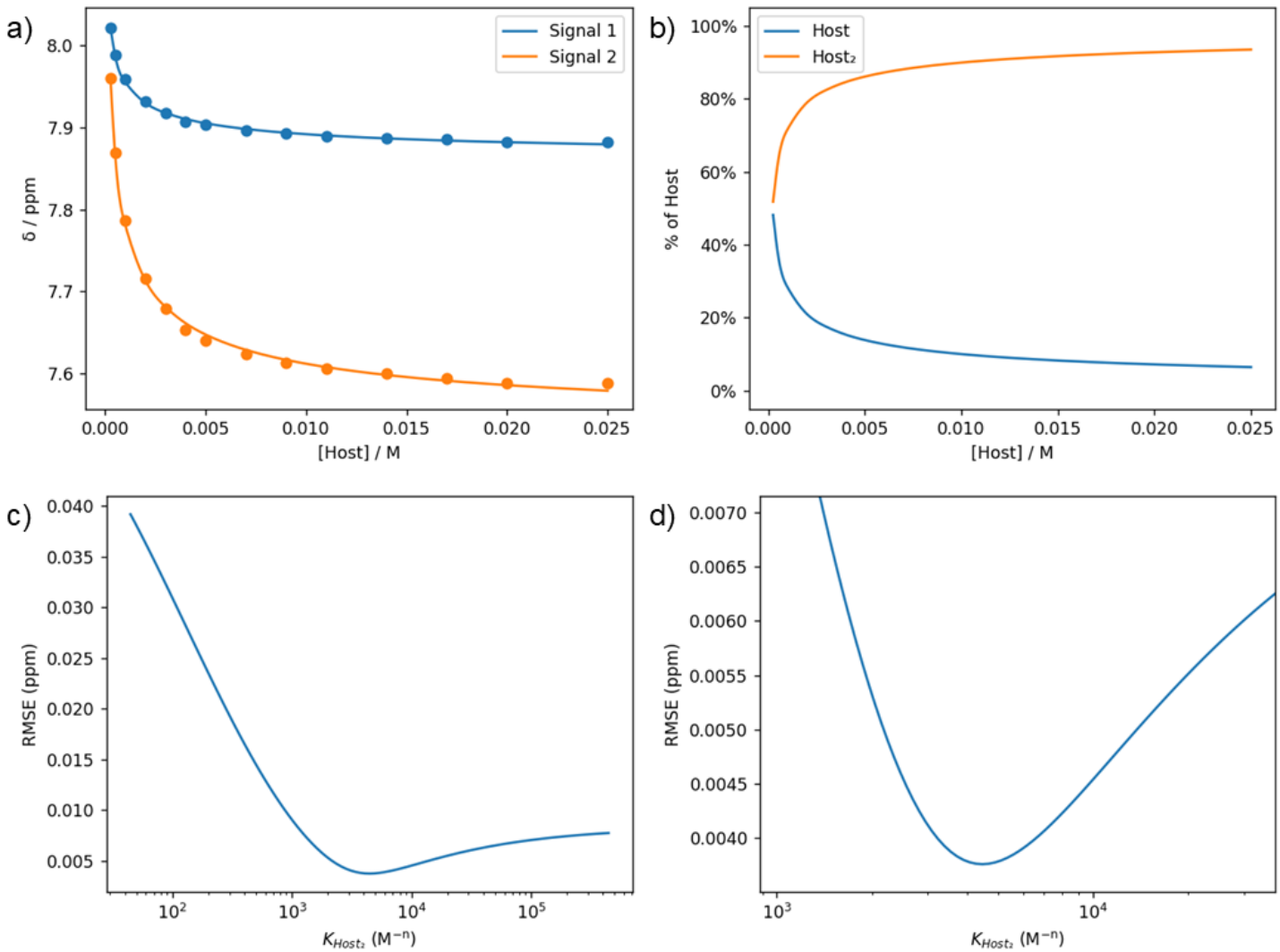


**Figure S12.** Fitting of data for self–association of **3** calculated using *Musketeer*:[8] a) fitting of peak movements (Signal 1 = interior phenylene resonance, Signal 2 = triazole resonance); b) speciation plot; c) error analysis plot showing calculated root mean square error (RMSE) against association constant; d) zoomed-in error analysis plot. Calculated $K_{dimerisation}$ = 4460 $M^{-1}$, RMSE = 0.0037.

**Self–association of 5:** Solution self–association of model compound **5** was studied in $CDCl_3$, $d_6$-acetone and 9:1 v:v $CDCl_3$:$d_6$-acetone. In each case, $^1$H NMR spectra were collected at a range of concentrations. As can be seen in Figures S13 and S14, no significant change in peak position is observed in either $CDCl_3$ or $d_6$-acetone over the range of concentrations studied. In 9:1 $CDCl_3$:$d_6$-acetone, significant changes are observed (Figures S15 and S16). The peak movements of the triazole C–H and internal phenylene C–H resonances (the peaks that moved the most) were fitted using a global fit in *Bindfit*[7] to give $K_{dimerisation}$ = 1361 ± 33 $M^{-1}$ (Figure S17). Fitting these same peaks in *Musketeer* gave $K_{dimerisation}$ of 1360 $M^{-1}$ (Figure S18).

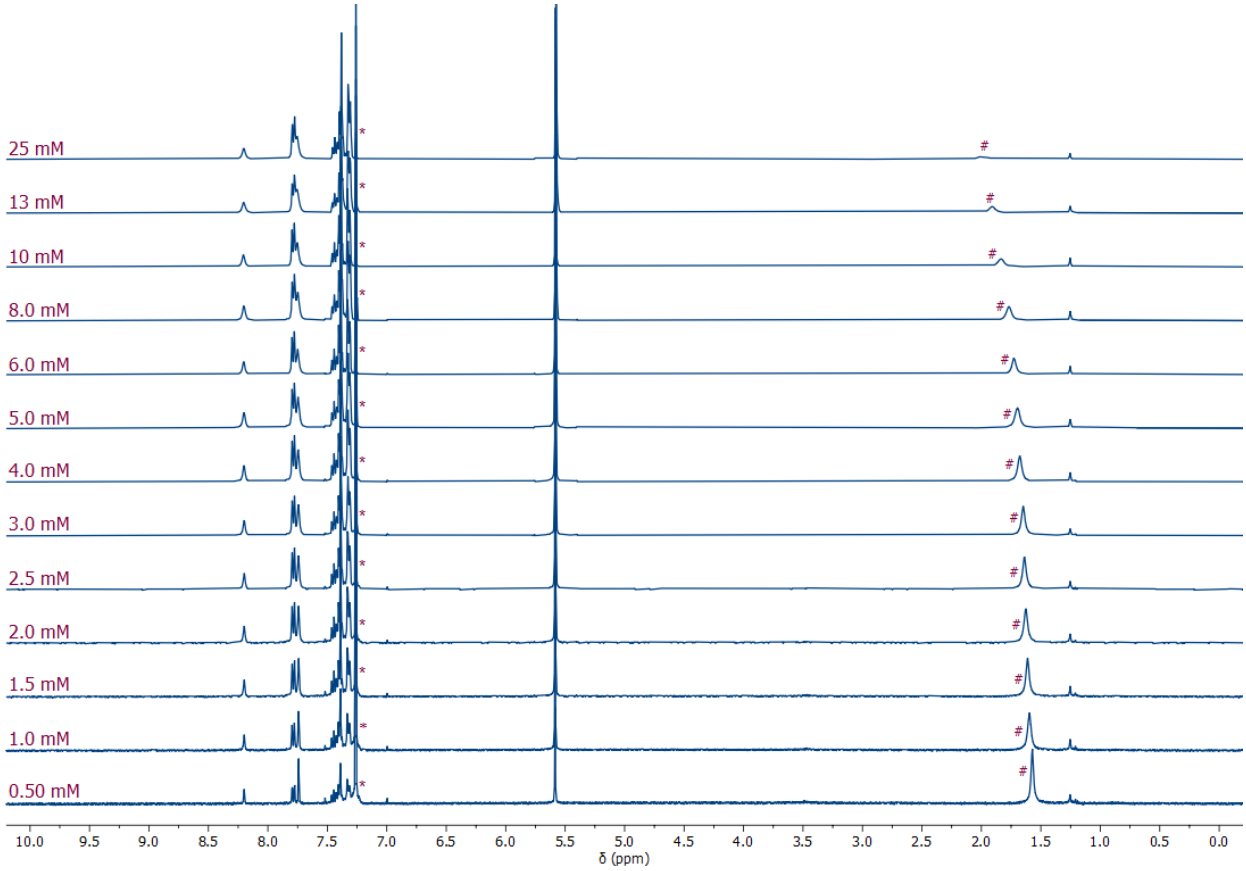


**Figure S13.** $^1$H NMR spectra of **5** at various concentrations in $CDCl_3$ (400 MHz, 298 K), * indicates incompletely deuterated NMR solvent peak, # indicates water.

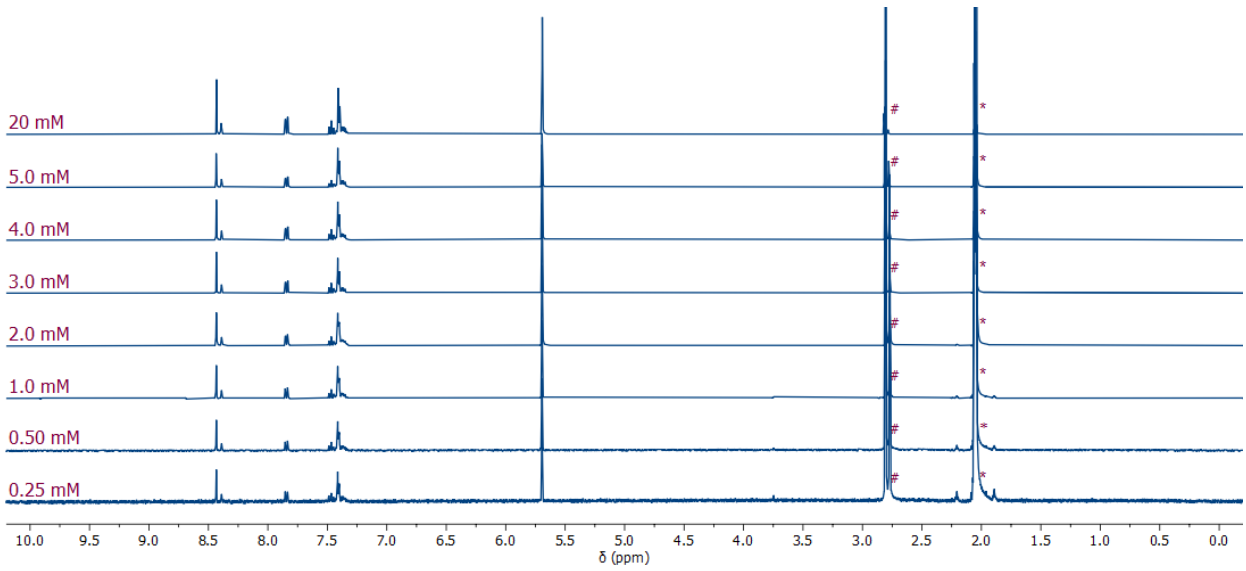


**Figure S14.** $^1$H NMR spectra of **5** at various concentrations in $d_6$-acetone (400 MHz, 298 K), * indicates incompletely deuterated NMR solvent peak, # indicates water.

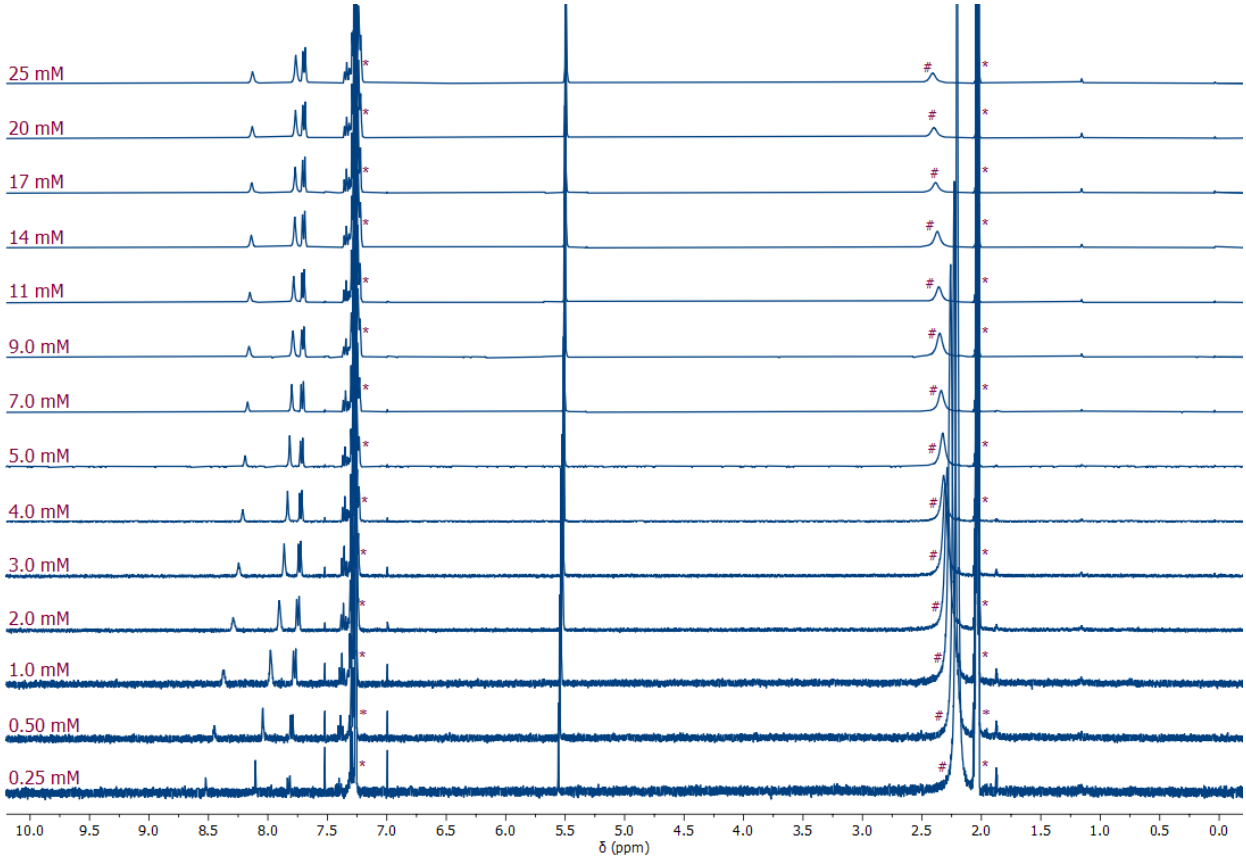


**Figure S15.** $^{1}$H NMR spectra of **5** at various concentrations in 9:1 $CDCl_3$:$d_6$-acetone (400 MHz, 298 K), * indicates incompletely deuterated NMR solvent peaks, # indicates water.

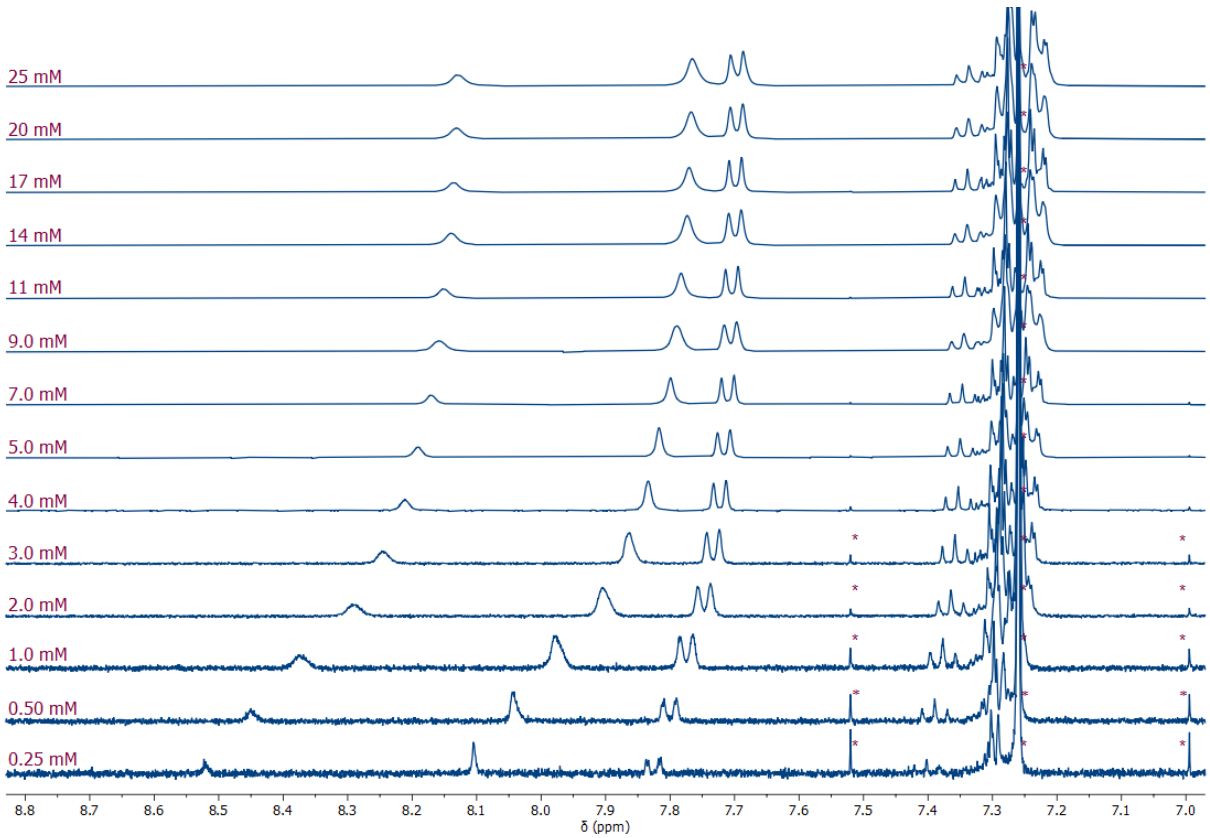


**Figure S16.** Partial $^{1}$H NMR spectra of **5** at various concentrations in 9:1 $CDCl_3$:$d_6$-acetone (400 MHz, 298 K), * indicates incompletely deuterated NMR solvent peak and $^{13}$C satellite peaks of this peak.

Full binding data including the calculated fit for this experiment can be obtained at:
http://app.supramolecular.org/bindfit/view/c68dd741-1b20-4acd-9ab4-35fb1d6375df

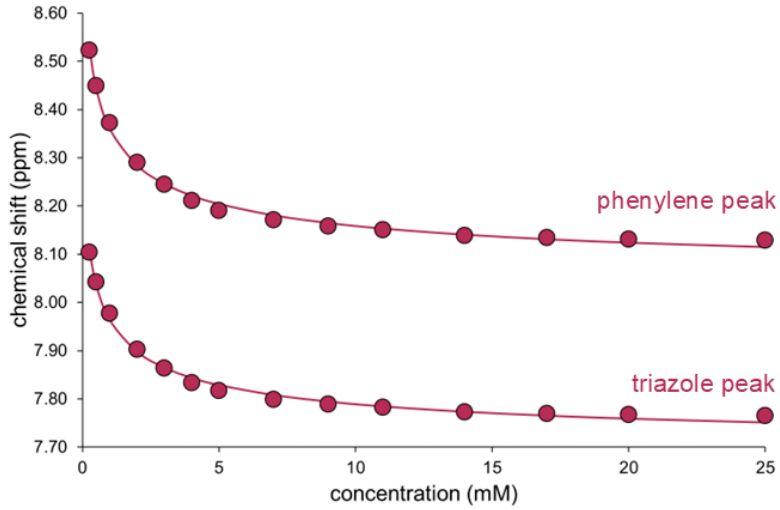


**Figure S17.** Chemical shift of interior phenylene and triazole C–H resonances at various concentrations; circles represent data, lines represent dimerization isotherm calculated using *Bindfit*[7] ($K_{dimerisation}$ = 1361 ± 33 $M^{-1}$).

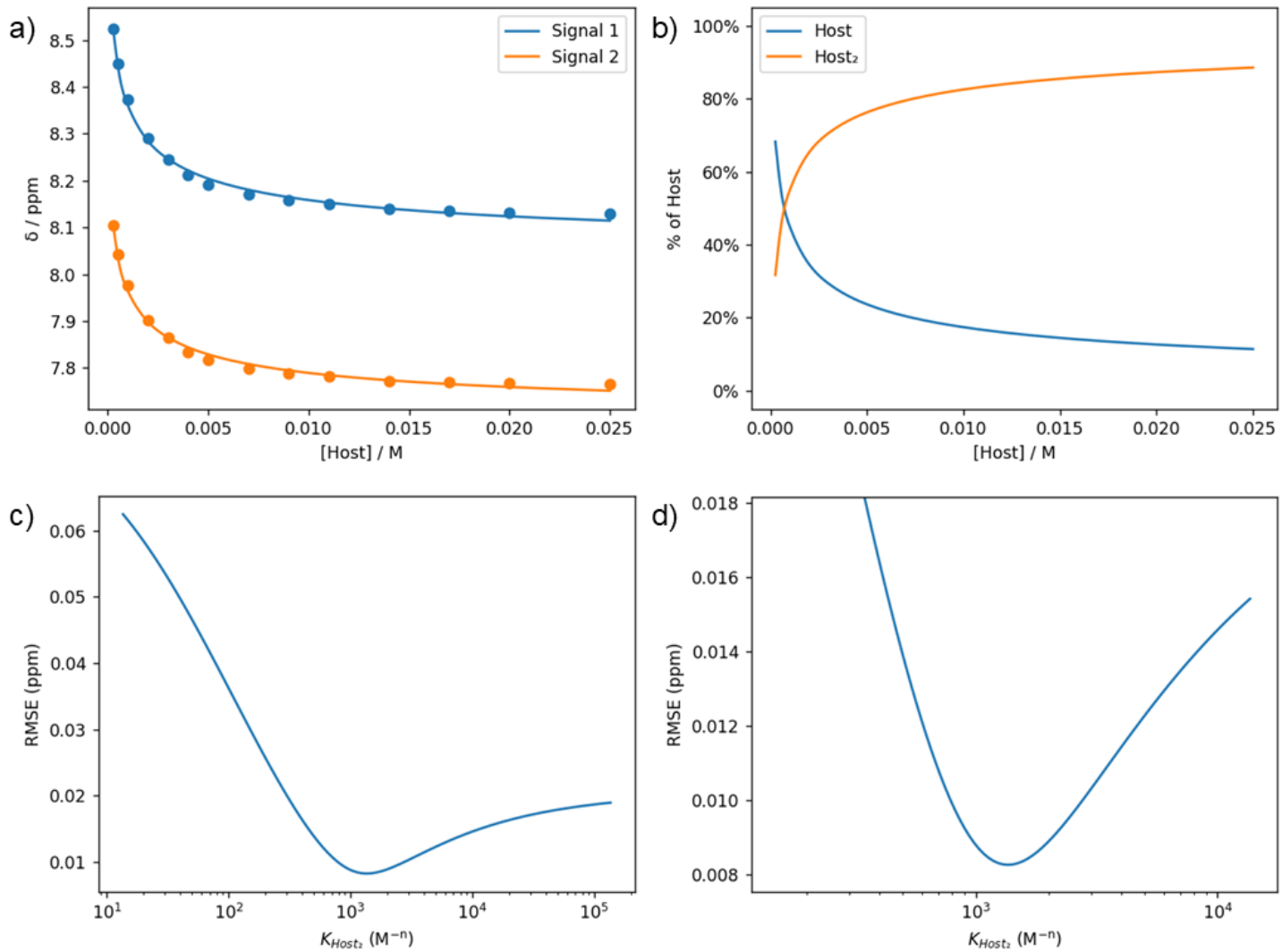


**Figure S18.** Fitting of data for self–association of **5** calculated using *Musketeer*:[8] a) fitting of peak movements (Signal 1 = interior phenylene resonance, Signal 2 = triazole resonance); b) speciation plot; c) error analysis plot showing calculated root mean square error (RMSE) against association constant; d) zoomed-in error analysis plot. Calculated $K_{dimerisation}$ = 1360 $M^{-1}$, RMSE = 0.0083.

**Self–association of 6:** Solution self–association of **btp** compound **6** was studied in $CDCl_3$, $d_6$-acetone and 9:1 v:v $CDCl_3$:$d_6$-acetone. In each case, $^1$H NMR spectra were collected at a range of concentrations. As can be seen in Figures S19 and S20, no significant change in peak position is observed in either $CDCl_3$ or $d_6$-acetone over the range of concentrations studied. In 9:1 $CDCl_3$:$d_6$-acetone, significant changes are observed (Figures S21 and S22). The peak movements of the triazole C–H and both pyridine C–H resonances (the peaks that moved the most) were fitted using a global fit in *Bindfit*[7] to give $K_{dimerisation}$ = 88486 ± 4273 $M^{-1}$ (Figure S23). Fitting these same peaks in *Musketeer* gave $K_{dimerisation}$ of 88500 $M^{-1}$ (Figure S24). While the estimated error on the value provided by *Bindfit* is of a sensible magnitude (~ 5%), we note that a dimerisation constant this strong is too high to be determined accurately using $^1$H NMR titrations, and the fits of the binding data are not perfect (Figures S23 and S24). As the *Musketeer* error analysis plots (Figure S24c and d) show, there is very little difference in RMSE for a value anywhere between 3 × $10^4$ $M^{-1}$ and $10^7$ $M^{-1}$. To err on the side of caution, we report this value in the main text as ~ $10^5$ $M^{-1}$. It is clear that **btp** dimerisation is significantly stronger in this solvent mixture than either that of either **3** or **5**.

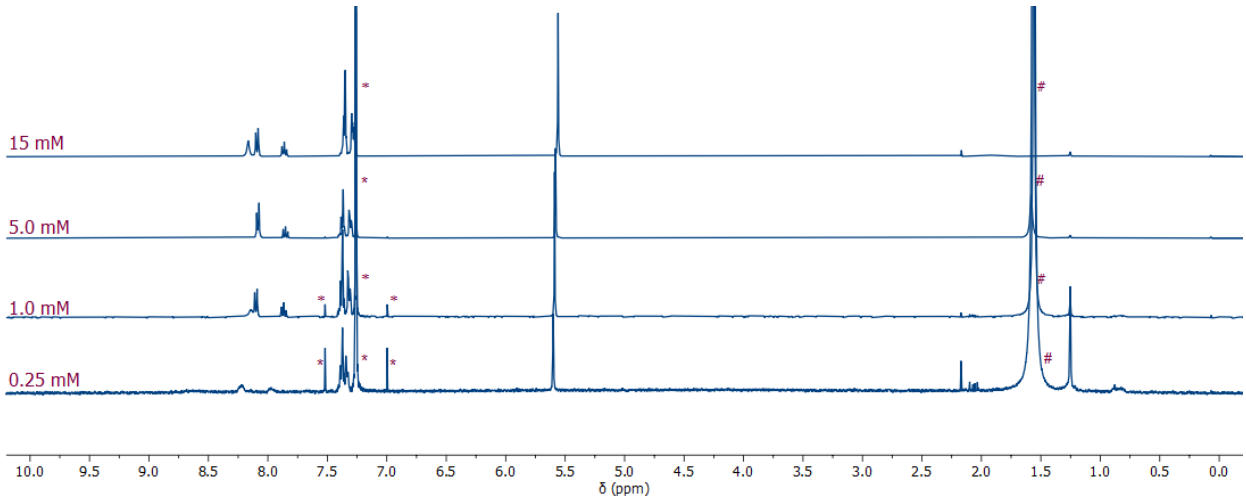


**Figure S19.** $^1$H NMR spectra of **6** at various concentrations in $CDCl_3$ (400 MHz, 298 K), * indicates incompletely deuterated NMR solvent peak or its satellites, # indicates water.

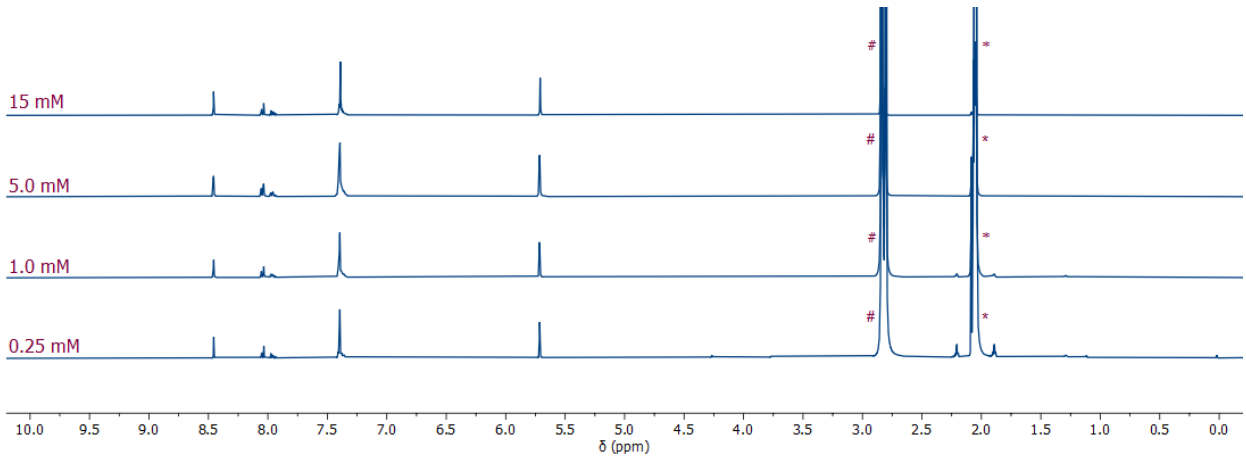


**Figure S20.** $^1$H NMR spectra of **6** at various concentrations in $d_6$-acetone (400 MHz, 298 K), * indicates incompletely deuterated NMR solvent peak, # indicates water. The highest concentration used was 15 mM due to limited solubility.

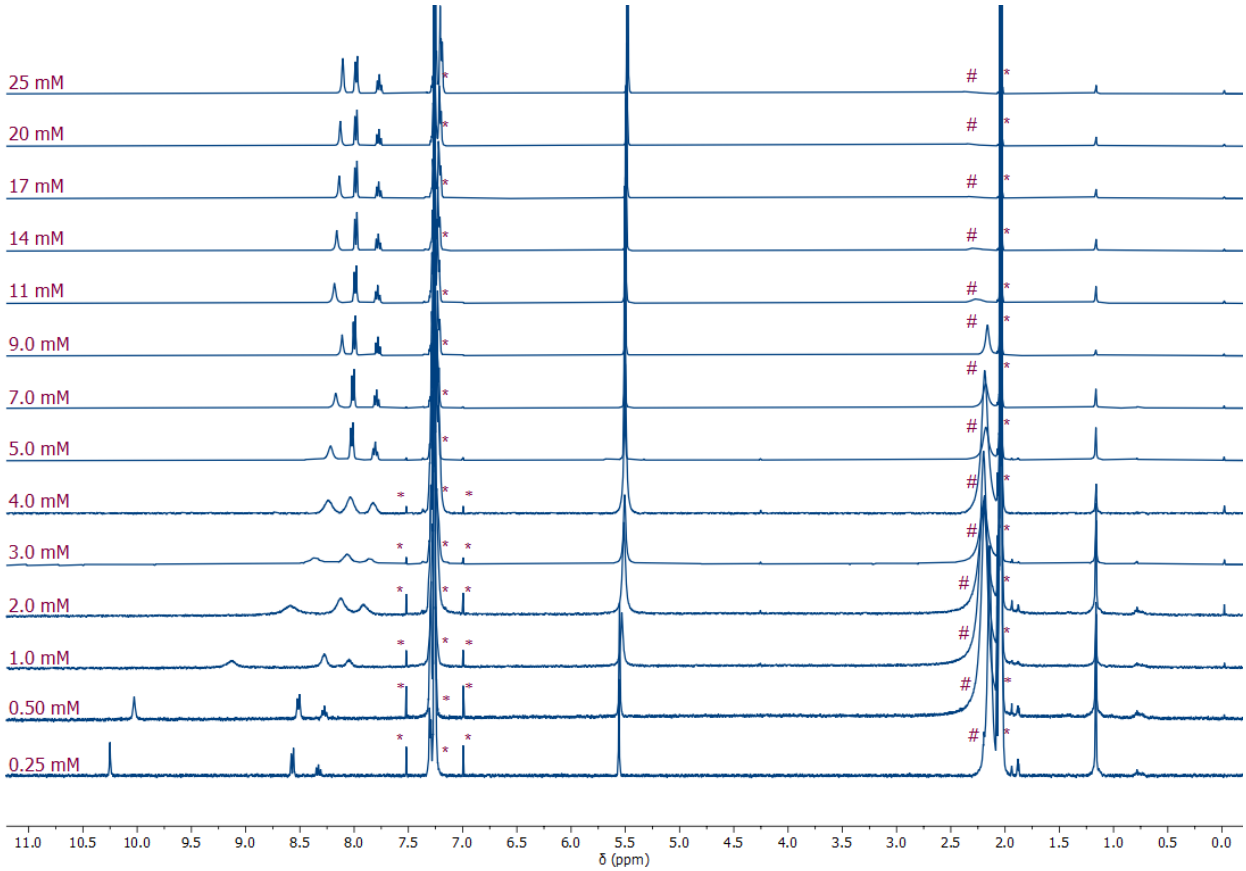


**Figure S21.** $^{1}$H NMR spectra of **6** at various concentrations in 9:1 $CDCl_3$:$d_6$-acetone (400 MHz, 298 K), * indicates incompletely deuterated NMR solvent peaks or its satellites, # indicates water. Peaks below 2.0 ppm are due to impurities in the NMR solvent used.

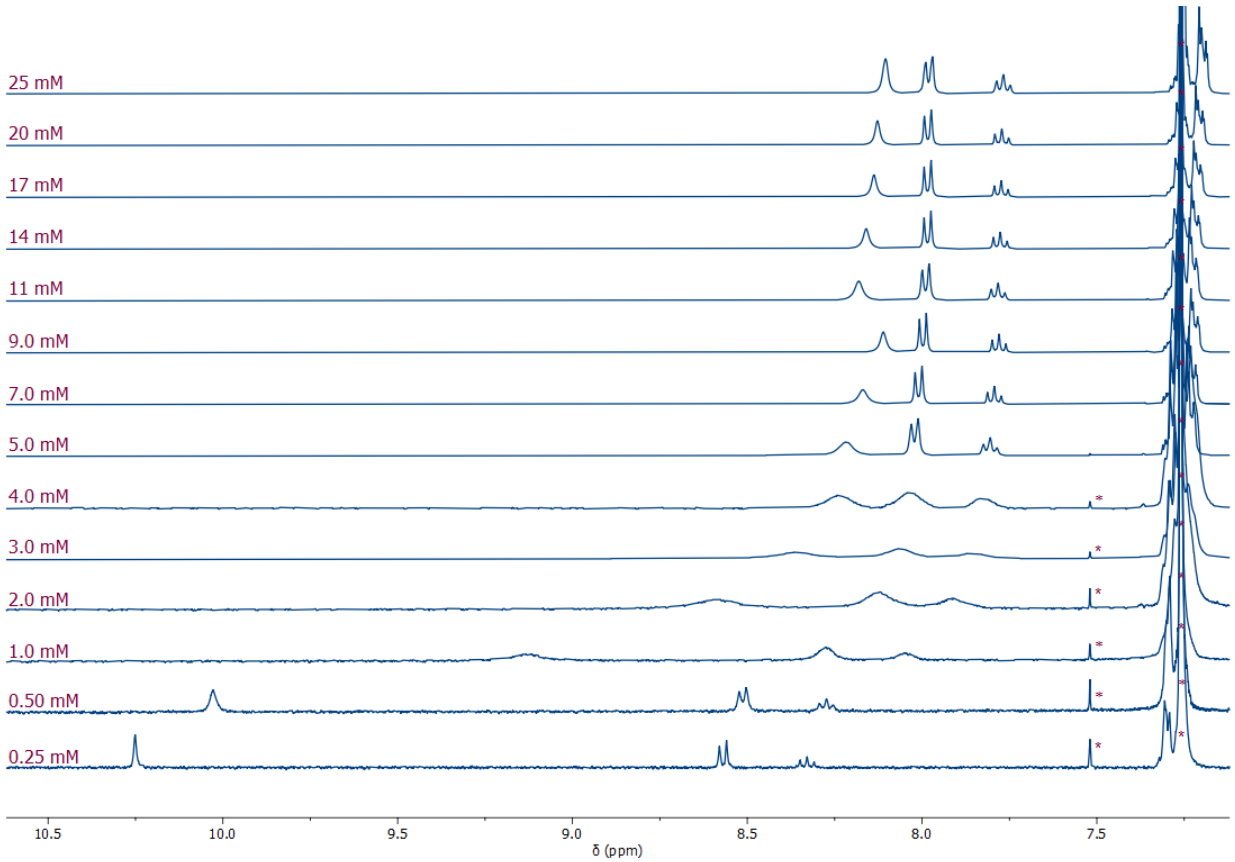


**Figure S22.** Partial $^{1}$H NMR spectra of **6** at various concentrations in 9:1 $CDCl_3$:$d_6$-acetone (400 MHz, 298 K), * indicates incompletely deuterated NMR solvent peak and $^{13}$C satellite peaks of this peak.

Full binding data including the calculated fit for this experiment can be obtained at:
http://app.supramolecular.org/bindfit/view/4e3bfe84-cdab-4f38-bf1a-f70b6d972834

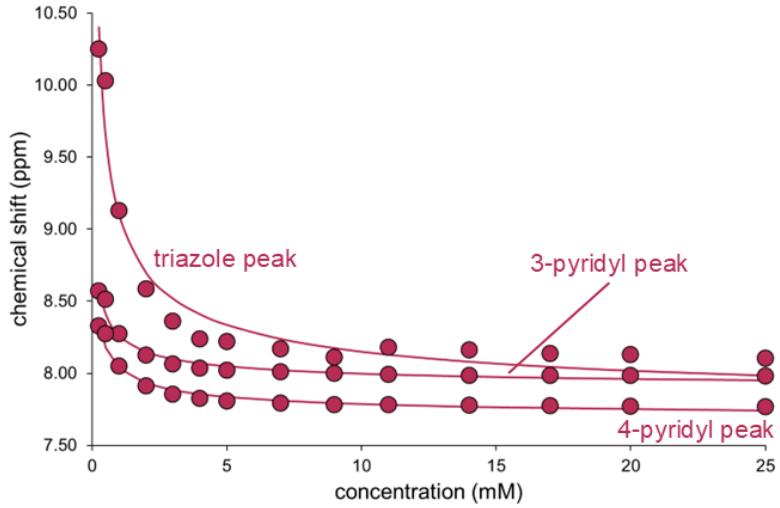


**Figure S23.** Chemical shift of interior phenylene and triazole C–H resonances at various concentrations; circles represent data, lines represent dimerization isotherm calculated using *Bindfit*[7] ($K_{dimerisation}$ = 88486 ± 4273 $M^{-1}$). Note curves fit relatively poorly and $K_{dimerisation}$ cannot be reliably determined due to strong binding.

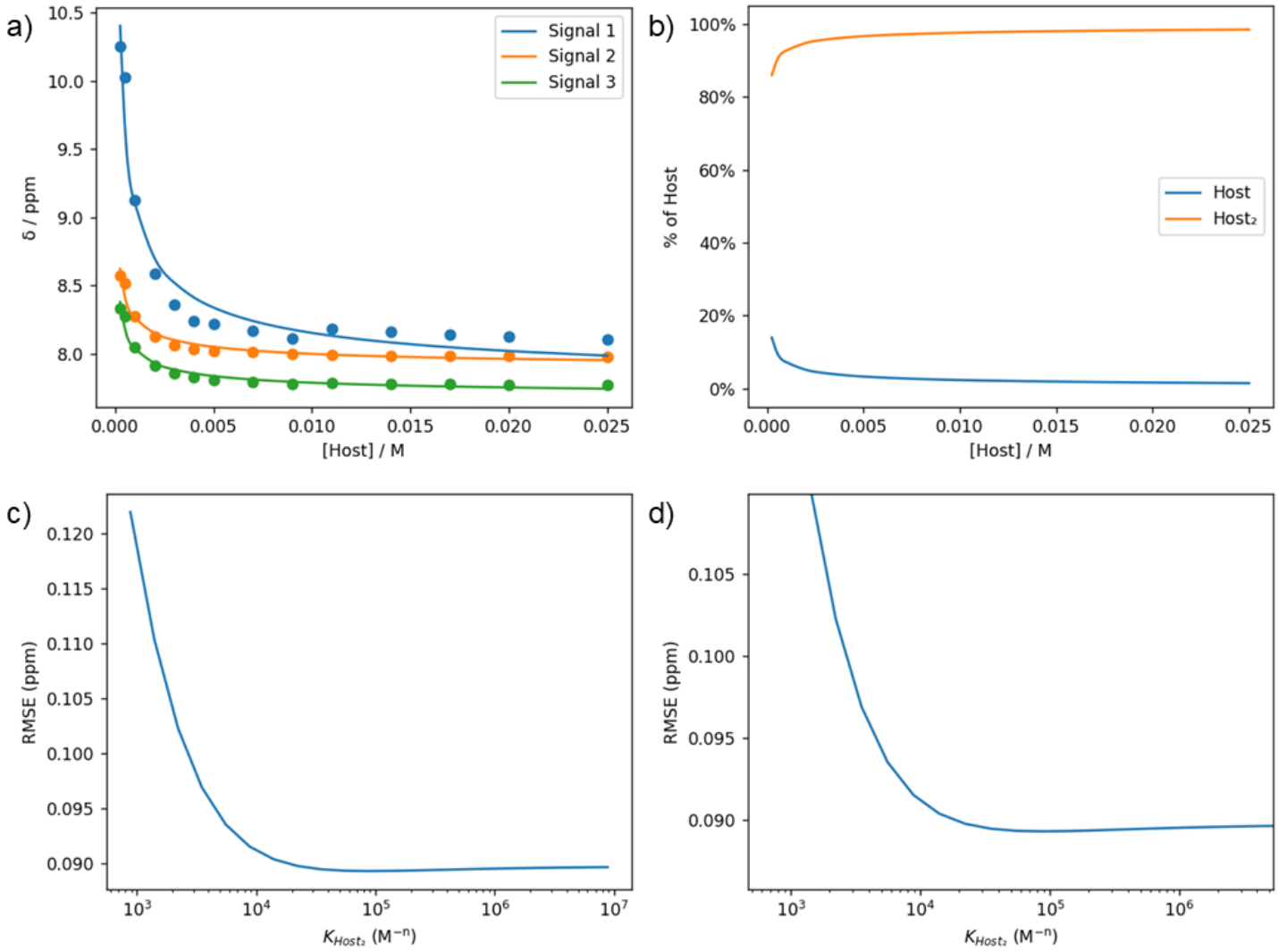


**Figure S24.** Fitting of data for self–association of **6** calculated using *Musketeer*:[8] a) fitting of peak movements (Signal 1 = triazole resonance, Signal 2 = 3-pyridyl resonance, Signal 3 = 4-pyridyl resonance); b) speciation plot; c) error analysis plot showing calculated root mean square error (RMSE) against association constant; d) zoomed-in error analysis plot. Calculated $K_{dimerisation}$ = 88500 $M^{-1}$, RMSE = 0.089. Note curves fit relatively poorly and $K_{dimerisation}$ cannot be reliably determined due to strong binding.

**Self–association of 7:** Solution self–association of model compound **7** was studied in $CDCl_3$ and 9:1 v:v $CDCl_3$:$d_6$-acetone. In each case, $^1$H NMR spectra were collected at a range of concentrations. As can be seen in Figure S25, no significant change in peak position is observed in 9:1 $CDCl_3$:$d_6$-acetone over the concentration range studied. Attempting to fit the very small shifts seen in this solvent to a dimerization process using *Bindfit*[7] resulted in $K_a << 1\ M^{-1}$. In $CDCl_3$, small changes in peak positions are observed (Figures S26 and S27). The peak movements of the phenylene C–H resonances (the peaks that moved the most) were fitted using a global fit in *Bindfit*[7] to give $K_{dimerisation} = 261 \pm 4\ M^{-1}$ (Figure S28). Fitting these same peaks in *Musketeer* gave $K_{dimerisation}$ of 261 $M^{-1}$ (Figure S29).

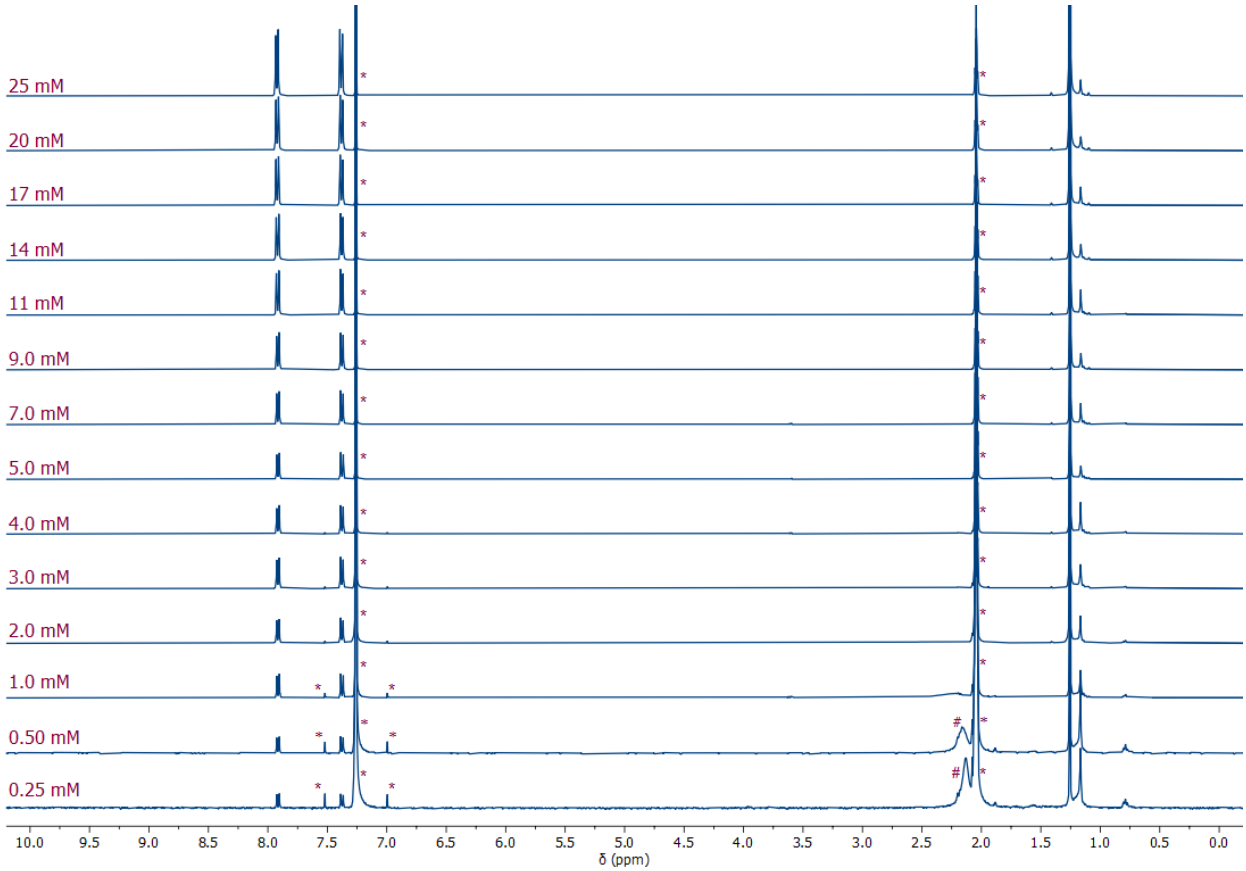


**Figure S25.** $^1$H NMR spectra of **7** at various concentrations in 9:1 $CDCl_3$:$d_6$-acetone (400 MHz, 298 K), * indicates incompletely deuterated NMR solvent peaks, # indicates water.

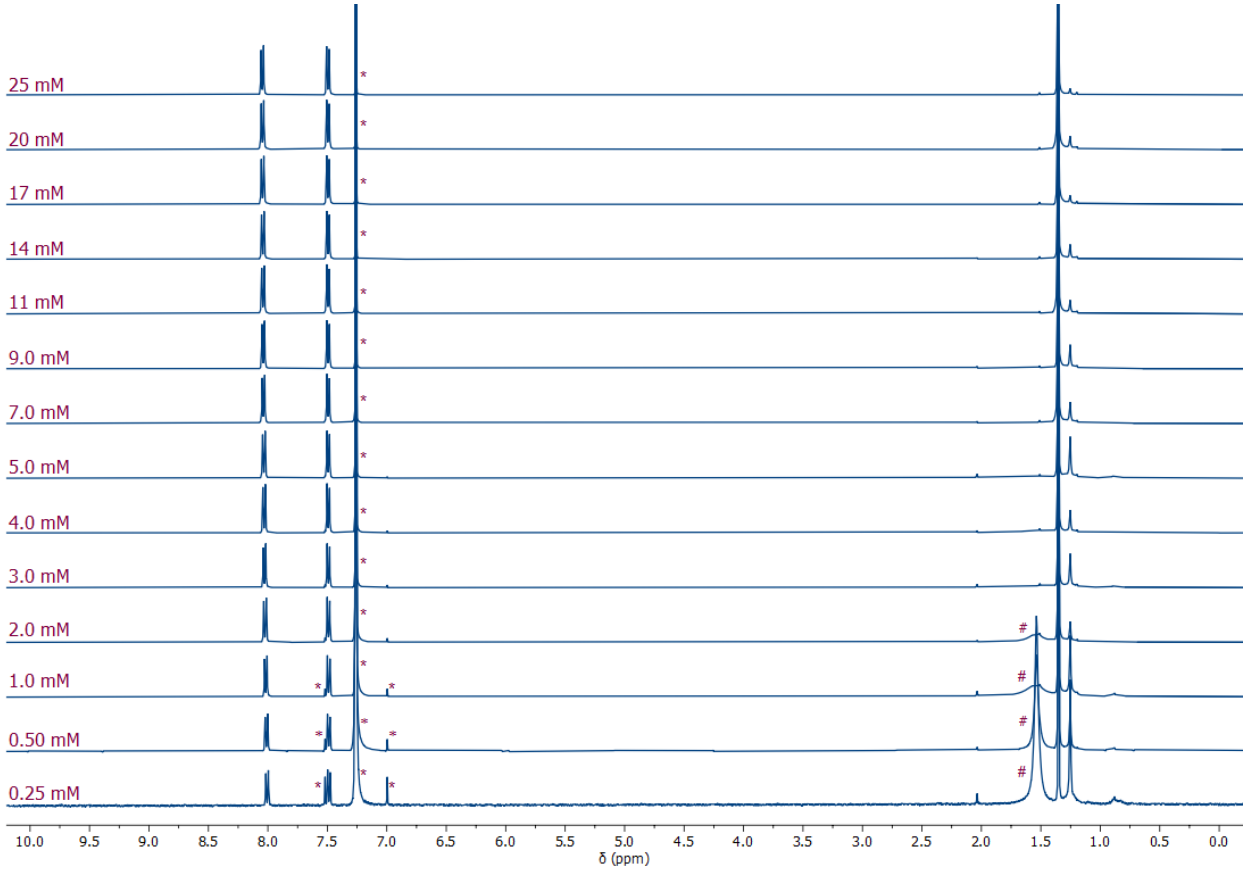


**Figure S26.** $^{1}$H NMR spectra of **7** at various concentrations in $CDCl_3$ (400 MHz, 298 K), * indicates incompletely deuterated NMR solvent peak, # indicates water.

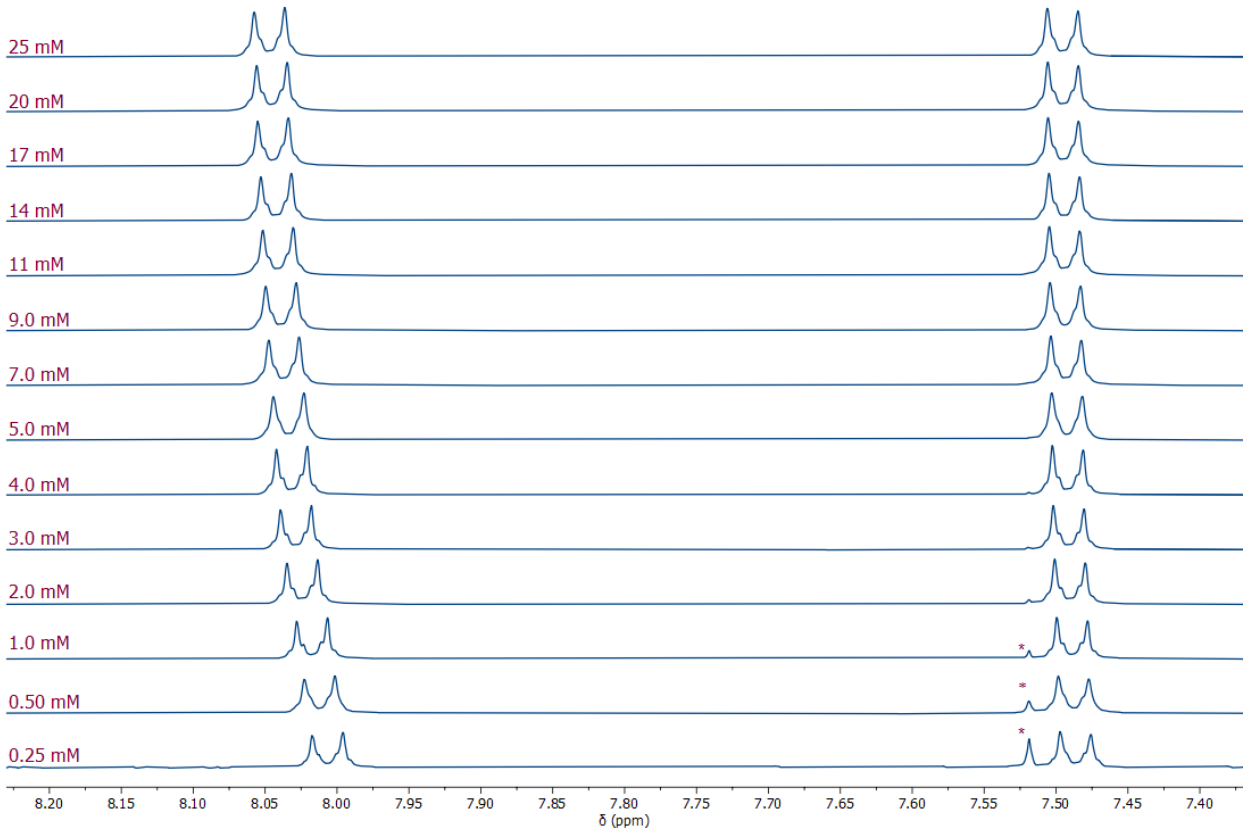


**Figure S27.** Partial $^{1}$H NMR spectra of **7** at various concentrations in $CDCl_3$ (400 MHz, 298 K), * indicates incompletely deuterated NMR solvent peak, # indicates water.

Full binding data including the calculated fit for this experiment can be obtained at:
http://app.supramolecular.org/bindfit/view/510f41a6-6710-432c-8bf3-4f0c5c15f658

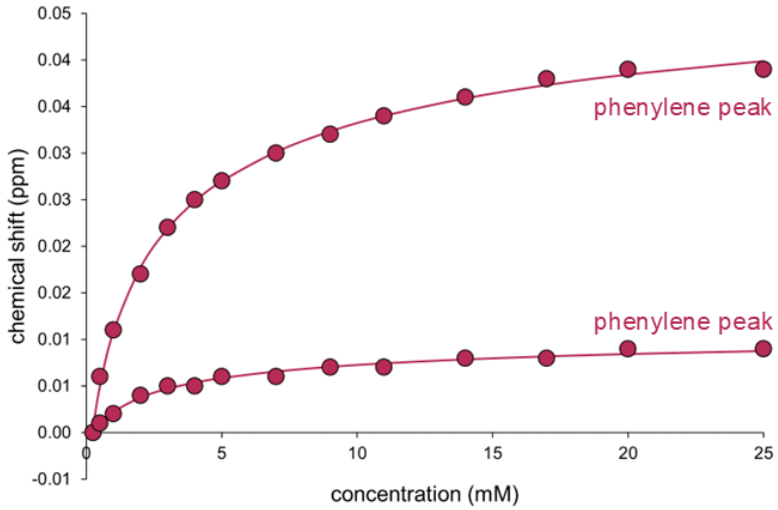


**Figure S28.** Chemical shift of interior phenylene C–H resonances at various concentrations; circles represent data, lines represent dimerization isotherm calculated using *Bindfit*[7] ($K_{dimerisation}$ = 261 ± 4 $M^{-1}$).

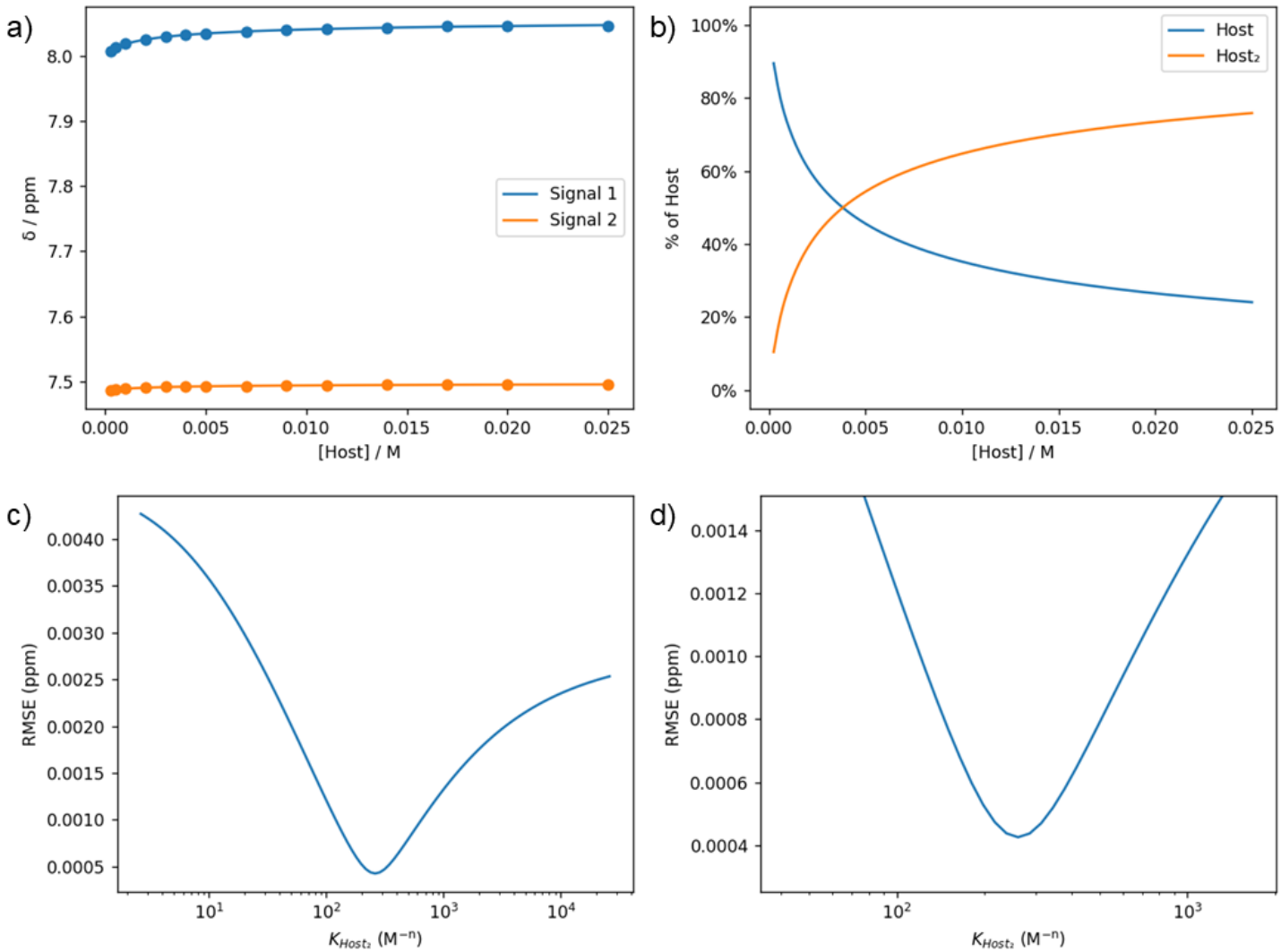


**Figure S29.** Fitting of data for self–association of **7** calculated using *Musketeer*:[8] a) fitting of peak movements (Signals 1 and 2 are the phenylene resonances of **6**); b) speciation plot; c) error analysis plot showing calculated root mean square error (RMSE) against association constant; d) zoomed-in error analysis plot. Calculated $K_{dimerisation}$ = 261 $M^{-1}$, RMSE = 0.0043.

## 3. X-RAY CRYSTALLOGRAPHY

Diffraction data were collected on an Oxford Diffraction SuperNova instrument using Cu radiation at 150 K. Raw frame data (including data reduction, interframe scaling, unit cell refinement and absorption corrections) were processed using CrysAlis Pro.[9] The structures were solved using SHELXT[10] and refined with SHELXL[11] within the OLEX2 suite.[12] All non-hydrogen atoms were modelled with anisotropic displacement parameters, and all hydrogen atoms were inserted at calculated positions using AFIX commands.

Details of any non-standard refinements are provided for each structure in the following section, along with thermal ellipsoid plots.

The data are summarised in Table S1. Full crystallographic data in CIF format have been deposited with the Cambridge Crystallographic Data Centre (CCDC Numbers: 2373363 – 2373366).

**Structure of $\mathbf{1}_{DCM/pentane}$:** Crystals were grown by vapour diffusion of pentane into a solution containing **1** and tetrabutylammonium chloride in dichloromethane. The asymmetric unit contains one half of a molecule of **1**, and one dichloromethane solvent molecule. Refinement proceeded smoothly and it was not necessary to use any crystallographic restraints.

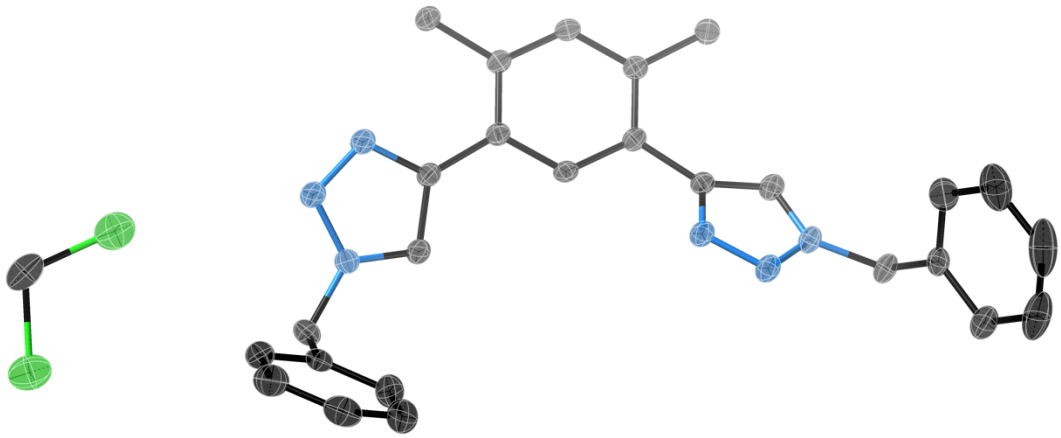

**Figure S30**. Thermal ellipsoid plot showing the asymmetric unit of $\mathbf{1}_{DCM/pentane}$. Ellipsoids shown at 50% probability, hydrogen atoms omitted for clarity.

**Structure of $\mathbf{1}_{workup}$:** The oily crude reaction mixture of **1** obtained following extraction and rotary evaporation yielded some crystals upon standing. This phase contained dichloromethane from work-up as well as some *t*-butanol from the reaction. The asymmetric unit contains one half of a molecule of **1**, and a region of ill-defined electron density. This could not be modelled sensibly and so the OLEX2 mask routine[12] was used to include this electron density in the refinement (292 electrons removed from a total volume of 1171 Å$^3$ in the unit cell, equivalent to ~ 36 electrons in the asymmetric unit or 73 electrons per molecule of **1**). Refinement proceeded smoothly and it was not necessary to use any crystallographic restraints.

Generally, the structure of $\mathbf{1}_{workup}$ is very similar to that of $\mathbf{1}_{DCM/pentane}$, although there are differences in the positions of the benzyl groups (Figure S31).

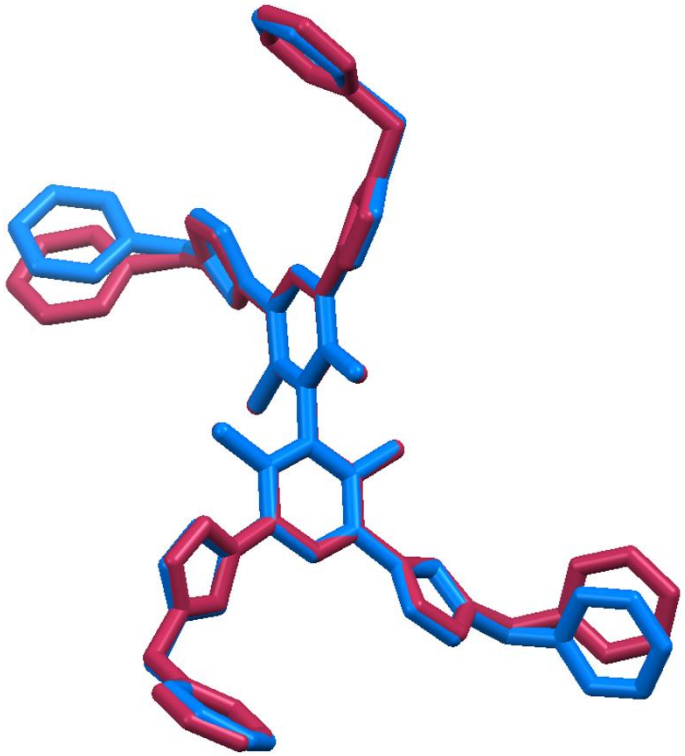

**Figure S31.** Overlay plot comparing X-ray crystal structure of $\mathbf{1}_{workup}$ with $\mathbf{1}_{DCM/pentane}$. The structure of $\mathbf{1}_{workup}$ is shown in red and the structure of $\mathbf{1}_{DCM/pentane}$ is shown in blue. Hydrogen atoms are omitted for clarity. Overlay calculated in Mercury.[13]

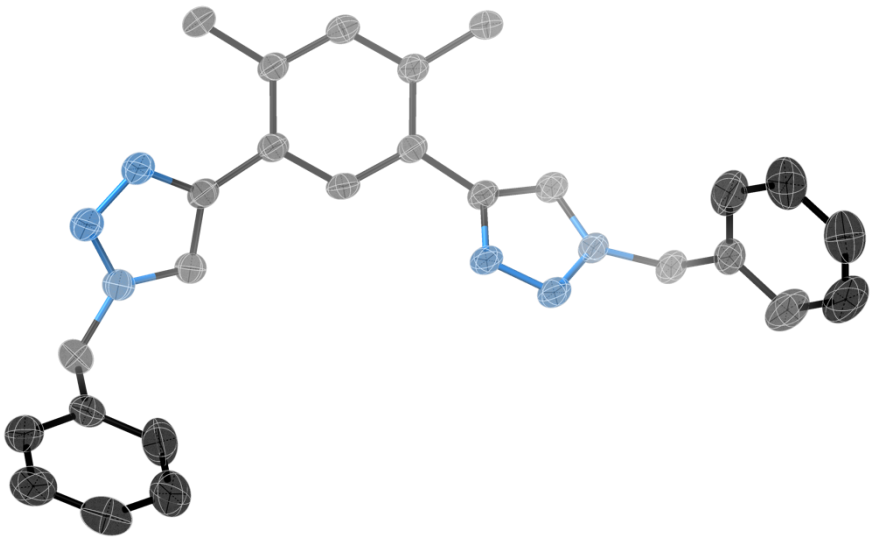

**Figure S32**. Thermal ellipsoid plot showing the asymmetric unit of $\mathbf{1}_{workup}$. Ellipsoids shown at 50% probability, hydrogen atoms omitted for clarity, OLEX2 mask routine[12] was used.

**Structure of $\mathbf{1}_{chloroform}$:** Crystals were grown by slow evaporation of a chloroform solution containing **1** and **5**. Crystals were relatively weakly-diffracting and it was only possible to obtain diffraction data to a resolution of 0.87 Å; despite this, the structure refines well. The crystals crystallise in the non-centrosymmetric space group $P2_1$ and the molecules in the crystal have axial chirality due to non-equivalent arrangements of benzyl triazole parts of the molecules. The Flack parameter is ambiguous, likely due to the fact that a full sphere of data was not collected, diffraction was relatively weak and there are few heavy atoms. The asymmetric unit contains two molecules of **1**, which differ in the conformations of the triazole groups, and four chloroform solvent molecules. Refinement proceeded smoothly and it was not necessary to add any crystallographic restraints.

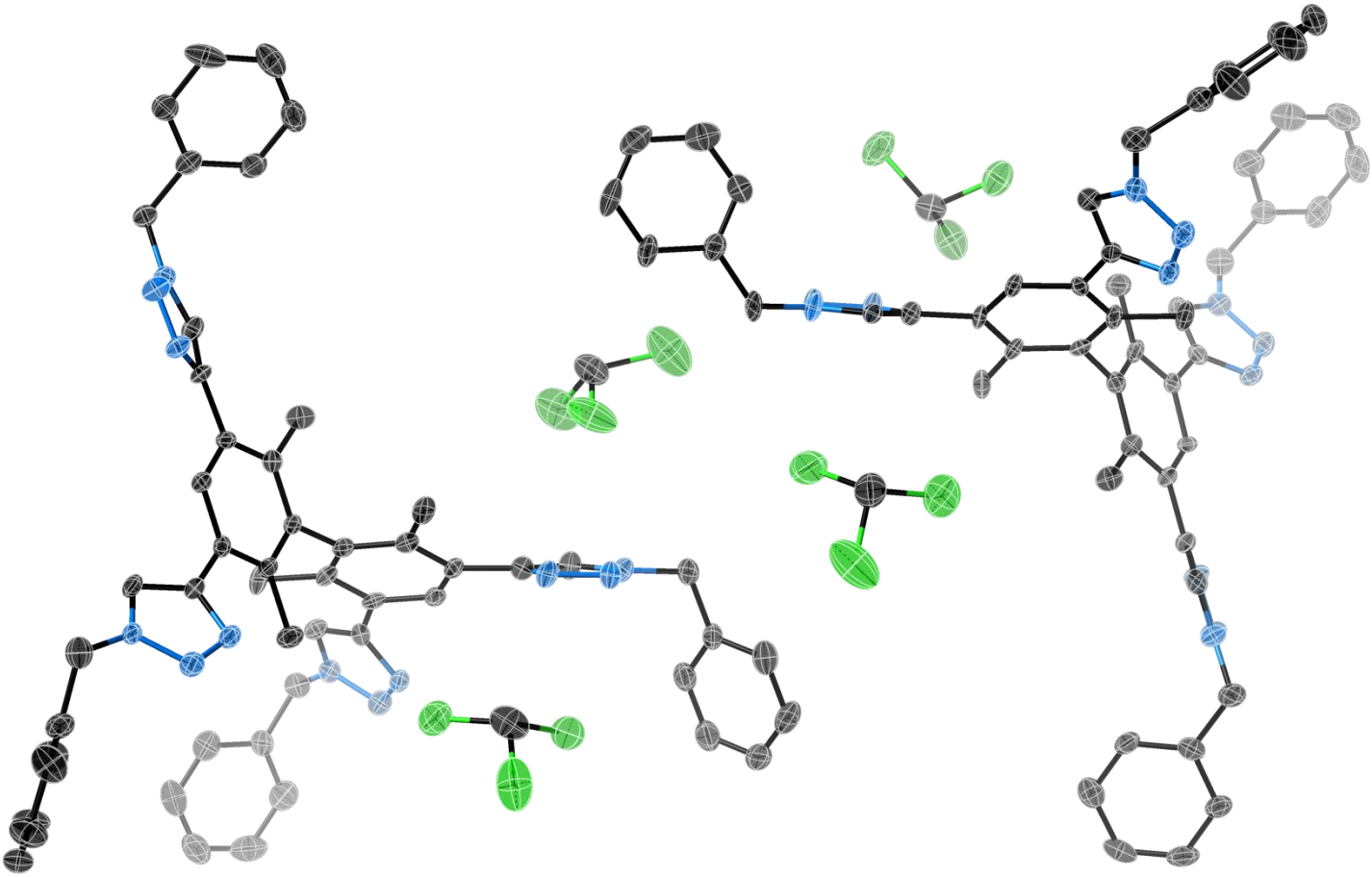

**Figure S33**. Thermal ellipsoid plot showing the asymmetric unit of $\mathbf{1}_{chloroform}$. Ellipsoids shown at 50% probability, hydrogen atoms omitted for clarity.

**Structure of $\mathbf{1}_{DCM/ether}$:** Crystals were grown by vapour diffusion of diethyl ether into a solution containing **1** and the tetrabutylammonium salt of tetrakis(carboxyphenyl)methane[14] in dichloromethane. Only crystals of **1** were obtained. These crystallise in the non-centrosymmetric space group P1, and the molecules in the crystal have axial chirality due to non-equivalent arrangements of benzyl triazole parts of the molecules. The Flack parameter is ambiguous, likely due to the fact that a full sphere of data was not collected and the absence of heavy atoms. The asymmetric unit contains one molecule of **1**, and a region of ill-defined electron density. This could not be modelled sensibly and so the OLEX2 mask routine[12] was used to include this electron density in the refinement (80 electrons removed from a total volume of 292 Å$^3$ in the P1 unit cell, *i.e.* 80 electrons per molecule of **1**). One of the benzylic phenyl rings is disordered; this was modelled over two positions (occupancies: 0.6:0.4) and it was necessary to use DFIX commands to restrain the C–C bond lengths of the two parts of the disorder to achieve a sensible refinement.

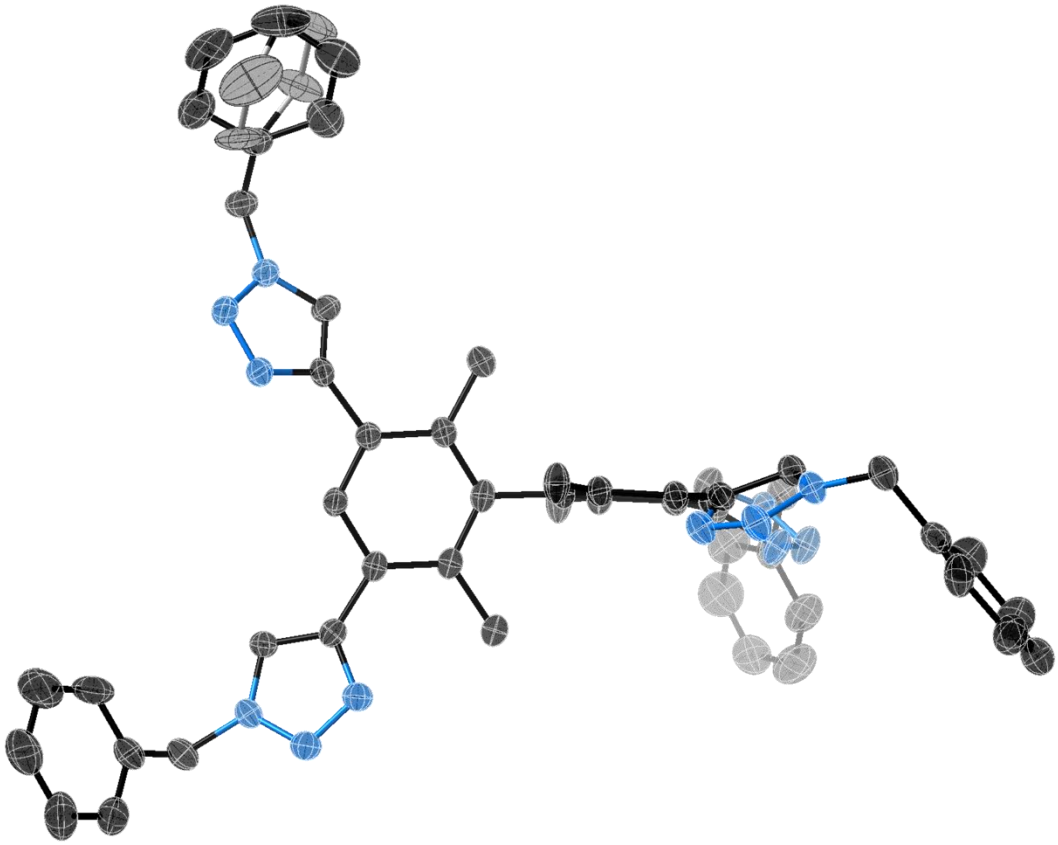

**Figure S34**. Thermal ellipsoid plot showing the asymmetric unit of $\mathbf{1}_{DCM/ether}$. Ellipsoids shown at 50% probability, hydrogen atoms omitted for clarity, OLEX2 mask routine[12] was used, lower occupancy part of disorder shown in pale grey.

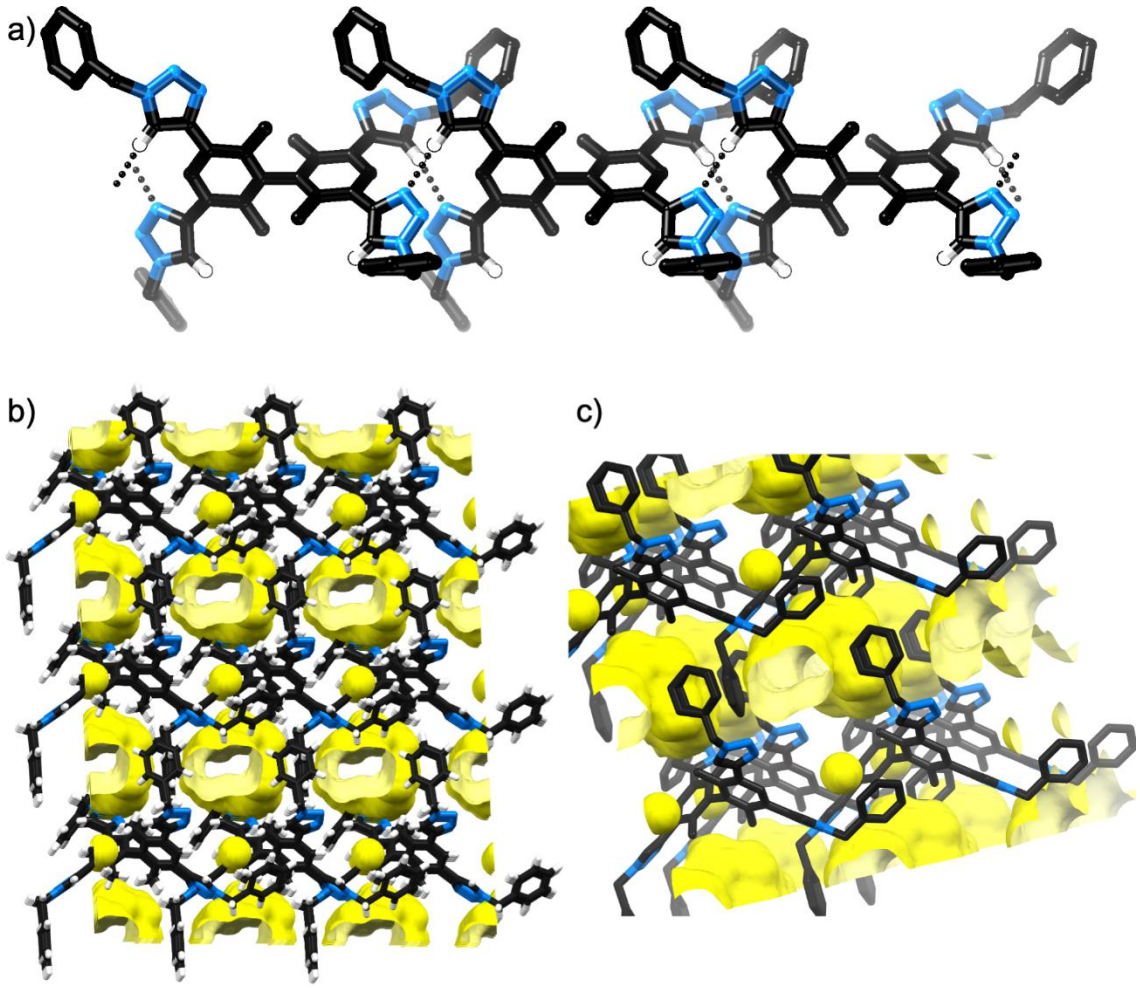


**Figure S35**. X-ray crystal structure of $\mathbf{1}_{DCM/ether}$: a) view of 1D hydrogen-bonded chain; b) view of channels in structure; c) close-up view showing helical channel structure. In some pictures, most or all hydrogen atoms are omitted for clarity, only the major position of the phenyl ring disorder is shown, OLEX2 solvent mask routine[12] was used.

**Table S1**. Summary of crystal structure data

| | $\mathbf{1}_{DCM/pentane}$ | $\mathbf{1}_{workup}$ | $\mathbf{1}_{chloroform}$ | $\mathbf{1}_{DCM/ether}$ |
|---|---|---|---|---|
| **CCDC No.** | **2373363** | **2373364** | **2373365** | **2373366** |
| Formula | $C_{52}H_{46}N_{12}\cdot2(CH_2Cl_2)$ | $C_{52}H_{46}N_{12}$ | $C_{52}H_{46}N_{12}\cdot2(CHCl_3)$ | $C_{52}H_{46}N_{12}$ |
| $M$ | 1008.86 | 839.01 | 1077.74 | 839.01 |
| $T$ (K) | 150 | 150 | 150 | 150 |
| Crystal system | monoclinic | monoclinic | monoclinic | triclinic |
| Space group | C2/c | C2/c | $P2_1$ | P1 |
| $a$ (Å) | 11.57630(10) | 11.4546(5) | 10.6444(3) | 10.8323(7) |
| $b$ (Å) | 18.4127(2) | 18.6173(7) | 49.4450(13) | 10.8523(10) |
| $c$ (Å) | 24.1317(3) | 24.6098(12) | 11.0340(4) | 13.3670(10) |
| $\alpha$ (°) | 90 | 90 | 90 | 68.942(8) |
| $\beta$ (°) | 103.2280(10) | 100.265(4) | 115.695(4) | 77.748(6) |
| $\gamma$ (°) | 90 | 90 | 90 | 63.780(8) |
| $V$ (Å$^3$) | 5007.22(10) | 5164.1(4) | 5233.1(3) | 1321.8(2) |
| $Z$ [$Z'$] | 4 [0.5] | 4 [0.5] | 4 [1] | 1 [1] |
| Crystal description | colourless block | colourless block | colourless block | colourless block |
| Crystal size (mm$^3$) | 0.25 × 0.18 × 0.10 | 0.16 × 0.09 × 0.03 | 0.14 × 0.11 × 0.04 | 0.29 × 0.24 × 0.06 |
| $\mu$ (mm$^{-1}$) | 2.550 | 0.525 | 3.394 | 0.517 |
| $\vartheta_{max}$, $\vartheta_{full}$ (°) | 66.594, 66.594 | 65.128, 65.128 | 62.385, 62.385 | 66.572, 66.572 |
| $N_{measured\ refl}$ | 13491 | 7145 | 15475 | 6788 |
| $N_{independent\ refl}$ [$R_{int}$] | 4415 [0.0131] | 4281 [0.0306] | 11518 [0.0525] | 4990 [0.0291] |
| $N_{observed\ refl}$ [$I > 2\sigma(I)$] | 4156 | 3200 | 9540 | 4741 |
| $N_{parameters}$ | 318 | 291 | 1305 | 618 |
| $N_{restraints}$ | 0 | 0 | 1 | 15 |
| $R_1$ [$I > 2\sigma(I)$] | 0.0343 | 0.0549 | 0.0715 | 0.0441 |
| $wR_2$ [all data] | 0.0914 | 0.1584 | 0.1850 | 0.1208 |
| GOF | 1.061 | 1.037 | 1.053 | 1.063 |
| OLEX2 mask routine[12] | – | 1171 Å$^3$ containing | – | 290 Å$^3$ containing |
| details (per unit cell) | | 292.4 e$^-$ | | 80.2 e$^-$ |
| $\Delta\rho_{max}$, $\Delta\rho_{min}$ (e Å$^{-3}$) | 0.24, –0.36 | 0.17, −0.23 | 0.88, −0.52 | 0.23, –0.23 |

## 4. CAMBRIDGE STRUCTURAL DATABASE SEARCHES

The Cambridge Structural Database (CSD)[15] Version 5.45 (November 2023) + one update was searched to find hydrogen bonds between 1,2,3-triazole C–H groups and either any neutral nitrogen atom, the N3-atom of another triazole group or the N2-atom of another triazole group using the search fragments shown in Figure S36. The data are presented in Table S2 and Figures S37 – S39.

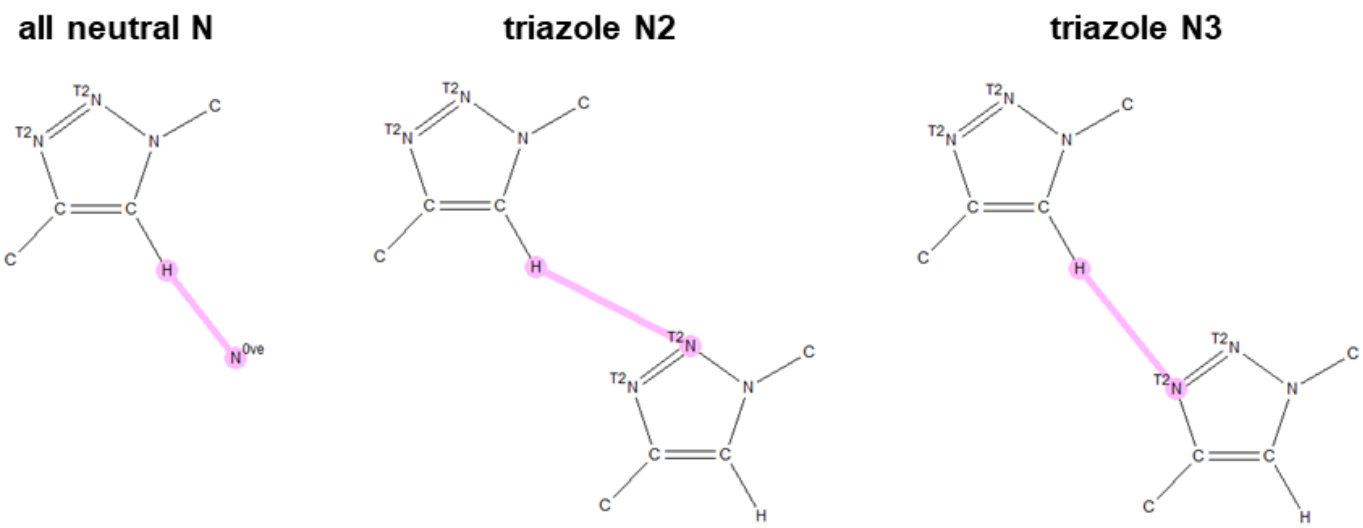


**Figure S36**. Search fragments used in CSD searches. A superscript "0ve" indicates that the atom was required to have zero charge. A superscript "T2" indicates that the nitrogen atom must be bound only to two other atoms (to avoid finding alkylated triazolium fragments or metal-coordinated triazole groups). In each case, the search was for a non-bonded contact between the H and N with a distance of 1.43 – 2.86 Å (50 – 100% of the sum of the van der Waals radii[16]).

**Table S2**. Summary of CSD hydrogen bonding data for the search fragments shown in Figure S36.

| | **triazole C–H ···all neutral N** | **triazole C–H ···triazole N2** | **triazole C–H ···triazole N3** | **this work[a]** |
|---|---|---|---|---|
| number of structures | 760 | 333 | 490 | 4 |
| number of close contacts | 1263 | 400 | 623 | 10 |
| shortest contact (Å) | 2.17 | 2.23 | 2.17 | 2.28 |
| longest contact (Å) | 2.86 | 2.86 | 2.86 | 2.49 |
| median contact (Å) | 2.61 | 2.63 | 2.61 | 2.39 |
| mean contact (Å) | 2.603 | 2.615 | 2.597 | 2.380 |
| standard error of mean (Å)[b] | 0.004 | 0.008 | 0.006 | 0.021 |
| 95% confidence interval of mean (Å) | 2.595 – 2.611 | 2.599 – 2.631 | 2.585 – 2.609 | 2.337 – 2.422 |

[a] C–H···N3 interactions involved in the "double" hydrogen bonding interactions only. [b] Estimated as the sample standard deviation divided by the square root of the number of close contacts.

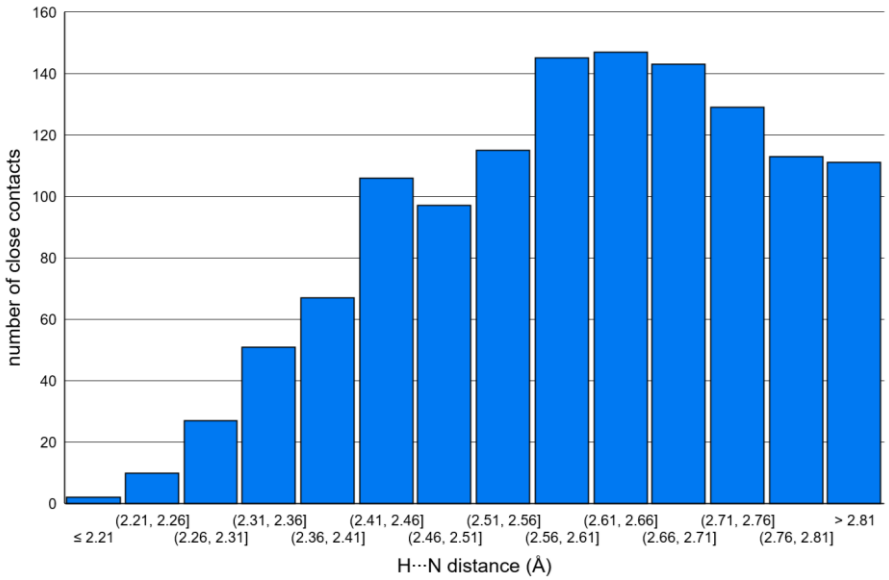


**Figure S37.** Histogram showing H···N contacts between triazole C–H hydrogen bond donors and any neutral nitrogen atom acceptor in the CSD.

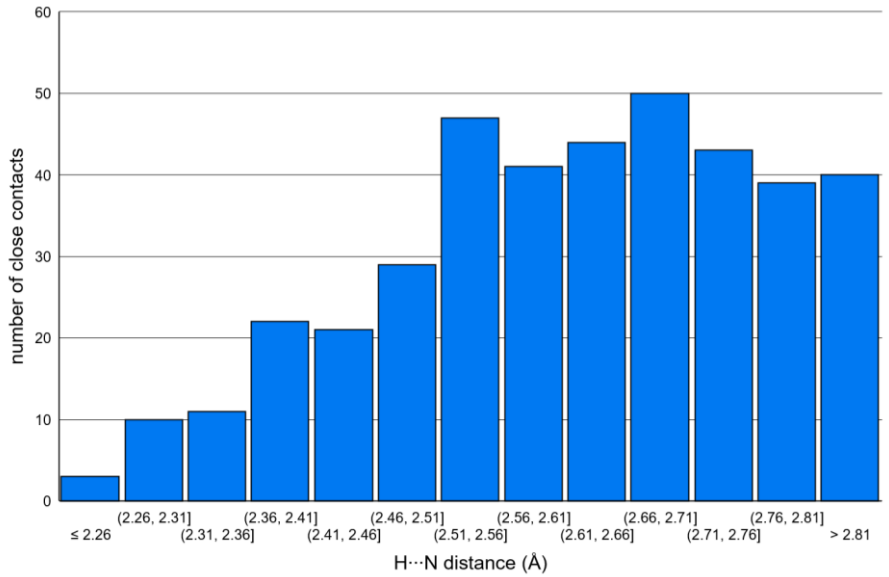


**Figure S38.** Histogram showing H···N contacts between triazole C–H hydrogen bond donors and triazole N2 acceptors in the CSD.

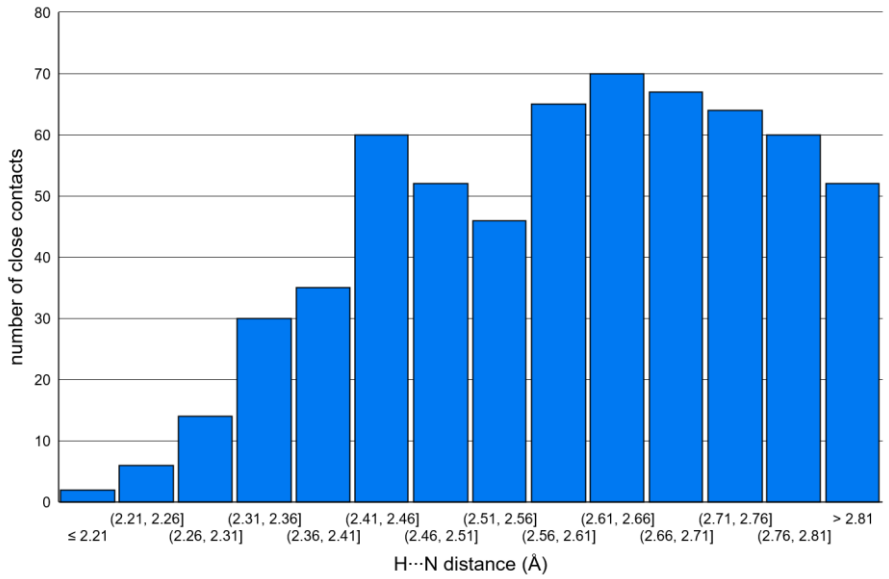


**Figure S39.** Histogram showing H···N contacts between triazole C–H hydrogen bond donors and triazole N3 acceptors in the CSD. Note that a version of this graph with the contacts from the structures reported in this work included in a different colour is shown in the main manuscript (Figure 5).

## 5. REFERENCES


[1] H. E. Gottlieb, V. Kotlyar, A. Nudelman, *J. Org. Chem.* **1997**, *62*, 7512–7515, https://doi.org/10.1021/jo971176v.

[2] S. Seth, G. Savitha, J. N. Moorthy, *Inorg. Chem.* **2015**, *54*, 6829–6835, https://doi.org/10.1021/acs.inorgchem.5b00722.

[3] B. Schulze, D. Escudero, C. Friebe, R. Siebert, H. Görls, S. Sinn, M. Thomas, S. Mai, J. Popp, B. Dietzek, L. González, U. S. Schubert, *Chem. Eur. J.* **2012**, *18*, 4010–4025, https://doi.org/10.1002/chem.201103451.

[4] E. J. O'Neil, K. M. DiVittorio, B. D. Smith, *Org. Lett.* **2007**, *9*, 199–202, https://doi.org/10.1021/ol062557a.

[5] M. L. Gower, J. D. Crowley, *Dalton Trans.* **2010**, *39*, 2371, https://doi.org/10.1039/B923211G.

[6] P. Danielraj, B. Varghese, S. Sankararaman, *Acta Crystallogr. C* **2010**, *66*, m366–m370, https://doi.org/10.1107/S010827011004223X.

[7] *Bindfit*, accessed at http://app.supramolecular.org/bindfit/.

[8] D. O. Soloviev, C. A. Hunter, *Chem. Sci.* **2024**, *15*, 15299–15310, https://doi.org/10.1039/D4SC03354J.

[9] *CrysAlis Pro*, Oxford Diffraction **2011**, https://rigaku.com/products/crystallography/x-ray-diffraction/crysalispro.

[10] G. Sheldrick, *Acta Crystallogr. Sect. A* **2015**, *71*, 3–8, https://doi.org/10.1107/S2053273314026370.

[11] G. M. Sheldrick, *Acta Crystallogr. Sect. C* **2015**, *71*, 3–8, https://doi.org/10.1107/S2053229614024218.

[12] O. V. Dolomanov, L. J. Bourhis, R. J. Gildea, J. A. K. Howard, H. Puschmann, *J. Appl. Crystallogr.* **2009**, *42*, 339–341, https://doi.org/10.1107/S0021889808042726.

[13] I. J. Bruno, J. C. Cole, P. R. Edgington, M. Kessler, C. F. Macrae, P. McCabe, J. Pearson, R. Taylor, *Acta Crystallogr. Sect. B* **2002**, *58*, 389–397, https://doi.org/10.1107/S0108768102003324.

[14] S. A. Boer, M. Morshedi, A. Tarzia, C. J. Doonan, N. G. White, *Chem. Eur. J.* **2019**, *25*, 10006–10012, https://doi.org/10.1002/chem.201902117.

[15] R. Taylor, P. A. Wood, *Chem. Rev.* **2019**, *119*, 9427–9477, https://doi.org/10.1021/acs.chemrev.9b00155.

[16] S. Alvarez, *Dalton Trans.* **2013**, *42*, 8617–8636, https://doi.org/10.1039/C3DT50599E.